ASTROPHYSICAL AND COSMOLOGICAL AXION BOUNDS

Master of Science thesis by
Sofie Vike Sivertsen
Institute of Theoretical Astrophysics
University of Oslo

August 2011

Abstract

The existence of dark matter is a well established fact both due to galaxy rotation curves and also due to the CMB temperature anisotropies and the matter power spectra. According to the ΛCDM model, the so called *standard model of cosmology*, 22% of the energy content of the Universe is in the form of dark matter. There are several dark matter candidates. In this thesis we will study one of them; the axion. The axion is well established from particle physics, introduced as the solution of the strong CP problem of Quantum Chromodynamics.

The aim of this work is to use astrophysics and cosmology to probe the properties of the axion. If axions are indeed present in stars, they will interact with the ordinary matter and thereby constitute a source of anomalous energy- loss. By studying the stellar evolution processes affected by this energy- loss, we can derive astrophysical bounds on the axion mass and coupling constant.

Axions present in the cosmic plasma of the early universe would *freeze- out* through the standard WIMP scenario. We compute the present axionic density parameter from this process and compare it with the density parameter for CDM obtained from the 7-year WMAP data, which results in a cosmological bound on the axion mass and decay constant.

Results obtained suggests an axion mass of order $m_a \sim O(\text{meV})$, hence a corresponding decay constant of order $f_a \sim O(10^{10}\,\text{GeV})$.

Acknowledgments

First of all I would like to thank my supervisor David F. Mota. Thank you for introducing me to this very interesting field of work. And also, just as importantly, for believing in me.

Next I would like to thank my Magnus and my daughter Ilma for keeping up with me and being supportive. Thanks also to my fellow students and the staff at ITA for the sharing of joy and frustration. Finally, I would also like to thank the rest of my family and friends for all the support during the writing of this thesis.

Sofie Vike Sivertsen
August 15, 2011

Contents

Chapter 1

Introduction

1.1 Stellar energy loss

One of the most prominent reasons for using stars to study particle physics is the impact on stellar evolution from the possible existence of a new weakly interacting low- mass particle.

This section is written mainly with the help of *Astrophysical methods to constrain axions and other novel particle phenomena*, ref. [1], but also the books of Carroll, ref. [2] and Prialnik, ref. [3] were useful references.

1.1.1 Stellar structure

To understand the impact of energy- loss mechanism from weakly interacting particles on the evolution of stars, we must understand the basic physics of stellar structure.

Equations of stellar structure

One usually assumes the star to be spherically symmetric and exclude effects such as rotation, magnetic fields and tidal effects from a binary companion[1]. There are four equations governing the stellar structure. The first equation is the assumption of *hydrostatic equilibrium*, i.e. that a spherical distribution of stellar meterial is held in place by opposing pressure and gravitational forces [2]:

$$\frac{dp}{dr} = -\frac{G\mathcal{M}_r\rho}{r^3}, \tag{1.1}$$

[1] A binary star system consists of two stars orbiting around their common center of mass.

[2] Note that one ignores the kinetic energy on the macroscopic level in the stellar medium, an assumption which is inadequate for processes such as supernova explosion and helium ignition (section 1.1.2).

where G is Newton's gravitational constant, p and ρ are the pressure and mass density at the radial position r. The mass $\mathcal{M}_r$ is the total mass inside the shell of radius r and it increases with radius according to

$$\frac{d\mathcal{M}_r}{dr} = 4\pi r^2 \rho, \tag{1.2}$$

known as the *mass- continuity equation*. For a star of radius R, the total mass is found by integrating this equation from the cent re, at $r = 0$, to the surface, at $r = R$.

Energy conservation yields another of the stellar structure equations. If the energy in- put balance the loss of energy in and out of a spherical mass shell, one finds

$$\frac{dL_r}{dr} = 4\pi r^2 \epsilon\, \rho.$$

Here L_r is the net flux of energy through a spherical shell of radius r while ϵ is the effective rate of local energy production. The latter is the sum

$$\epsilon = \epsilon_{nuc} + \epsilon_{grav} - \epsilon_{\mu} - \epsilon_x,$$

where ϵ_{nuc} is the rate by which nuclear energy is liberated, ϵ_{μ} is the energy- loss rate by standard neutrino production and ϵ_x is for novel particles. The equation,

$$\epsilon_{grav} = c_p T \left[\nabla_{ad} \frac{\dot{p}}{p} - \frac{\dot{T}}{T} \right],$$

gives the local energy gain when T and p change due to the expansion or contraction of the star. The quantity c_p is the heat capacity at constant pressure and ∇_{ad},

$$\nabla_{ad} \equiv \left(\frac{\partial \ln T}{\partial \ln p} \right)_s,$$

taken at constant entropy s is the *adiabatic temperature gradient*. The calculation of ϵ_x will be important in the derivation of bounds from anomalous energy- loss in chapter 3.

The transfer of energy in stars is driven by the radial temperature gradient. In the absence of convection heat is carried through radiative transfer by photons and also by electrons moving between regions of different temperature, i.e. through conduction. In this case the relationship between the energy flux and the temperature gradient is

$$L_r = -\frac{4\pi r^2}{3\,\kappa\rho} \frac{d\,(a\,T^4)}{dr},$$

where $a\,T^4$ is the energy stored in the radiation field[3] and κ is the *opacity*, which describes the absorption and scattering of radiation in a medium.

The viral theorem

In general, the pressure is given in terms of the density, temperature and chemical composition through an *equation of state*. For a classical monatomic gas $p = \frac{2}{3}\,u$, where u is the density of internal energy. If one multiplies eq. 1.1 on both sides by $4\pi r^3$ and integrate from the cent re to the surface, the right hand side gives the total gravitational energy. After a partial integration with the boundary condition $p = 0$ at the surface, the left hand side reveals -2U, with U the total internal energy of the star. For a monatomic gas, U is the sum of the kinetic energies of the atoms. One finds that on average for every atom

$$E_k = -\frac{1}{2}\,E_{grav}. \tag{1.3}$$

This is the well known *viral theorem* which is very important when studying self-gravitating systems.

Degeneracy pressure

There are two main sources of pressure relevant in stars, thermal pressure and degeneracy pressure. The third possibility, radiation pressure is only relevant in very massive stars. In a non-degenerate, nonrelativistic medium the pressure is

$$p \propto -\frac{\rho}{\mu}\,T,$$

where ρ is the mass density and T the temperature. Here μ is the mean molecular weight of the medium constituents. For nonrelativistic degenerate electrons the density is

$$n_e = \frac{p_F^3}{3\pi^2},$$

where p_F is the Fermi momentum[4]. A typical momentum is of size p_F, and the velocity is p_F/m_e, yielding a pressure which is proportional to p_F^5 or $n_e^{5/3}$ and thus

$$p \propto \rho^{5/3}. \tag{1.4}$$

A normal star is geometrically larger if it has a larger mass, i.e. $R \propto \mathcal{M}$. To find this relationship for degenerate conditions, we approximate the left hand side of the equation for hydrostatic equilibrium (eq. 1.1) as p/R and the right hand

[3] The Stefan Boltzmann law

[4] The Fermi momentum is associated to the Fermi energy which usually refers to the energy of the highest occupied quantum state in a system of fermions at absolute zero temperature.

side as $M\rho/R^2$. Comparing with the relation given in 1.4 reveals that the mass-radius relationship is inverted for a degenerate configuration, more specifically

$$R \propto M^{-1/3}. \tag{1.5}$$

The radius increases with increasing mass!

Further increase of mass beyond a certain limit causes the radius to shrink so much that the electrons become relativistic. Relativistic electrons move with a constant velocity of c and therefore special relativity must be taken into account. This leads the pressure to vary only as $\rho^{4/3}$. Adding more mass no longer leads to a sufficient pressure increase to balance the extra weight. This happens at a mass of about 1.4 $M_\odot$, and is known as the *Chandrasekhar limit*. Beyond this limit, no stable degenerate configuration exists.

1.1.2 Stellar evolution

There is much literature written on the subject of stellar evolution [5]. For the purpose of this thesis we only need to present a very brief introduction with emphasis on the energy loss argument.

Star formation

Stars form as gravitationally bound clouds of gas fragment and condense due to their energy loss by electromagnetic radiation. When the star radiates energy its total energy decreases. If it is roughly in an equilibrium configuration, the viral theorem in 1.3 tells us that a decrease in $(E_k + E_{grav})$ causes the gravitational energy to become more negative, corresponding to a more tightly bound system. The cloud therefore contracts and since it becomes more compact the average kinetic energy goes up. Assuming the system is in local thermal equilibrium, this leads to an increase in temperature. The conclusion is that self- gravitation systems that loose energy contract and heat up, and hence have negative specific heat.

Onset of nuclear fusion

Further contraction eventually causes the star to reach a high enough temperature for the onset of nuclear fusion of hydrogen. The essentials of this nuclear process is that four protons and two electrons combine to form a helium nucleus (α particle), releasing energy. Due to the steep temperature dependence of the nuclear reaction rates, a further contraction and heating of the star leads to an expansion and cooling by the same viral theorem logic that led to contraction

[5] Most of this theory is based on ref. [1], which on page 24 present a list of relevant textbooks and review articles on this subject.

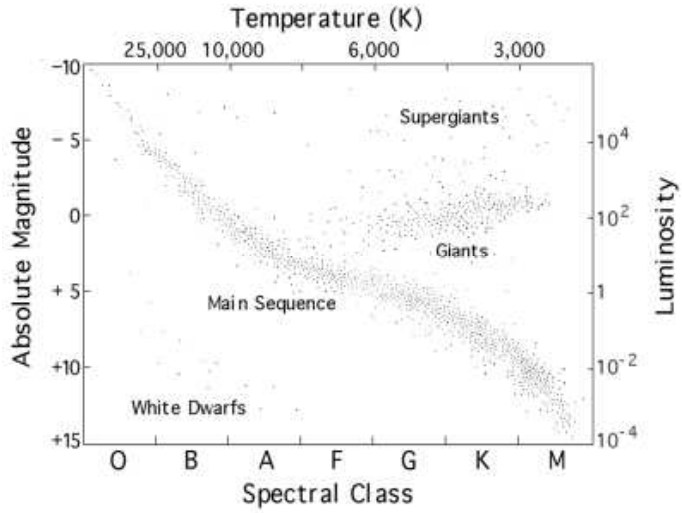

Figure 1.1: Hertzsprung- Russel diagram. Figure courtesy of NASA: http://heasarc.gsfc.nasa.gov/

and heating when energy was lost. Thus the star is now a stable configuration in thermal equilibrium where the energy lost by radiation is exactly balanced by that produced from nuclear reactions.

The most important feature of a normal stellar configuration is the interplay between the negative specific heat and the nuclear energy generation. However, in a star where the pressure is dominated by degeneracy pressure, it is independent of temperature. In this case these self- regulating effects would break down since heating would not lead to expansion. A configuration dominated by degeneracy pressure has positive heat capacity so that a loss of energy no longer implies contraction and heating. We can conclude that a star can only continue stable nuclear production as long as the thermal pressure dominates.

Main sequence

The new star will find its place on the so called *main sequence* in the Hertzsprung-Russel (HR) diagram, where the effective surface temperature is plotted on the horizontal axis and the stellar luminosity on the vertical axis. There it continues to fuse hydrogen for billions of years if it has a small mass ($\sim 1\,M_\odot$), while the supermassive stars leave the main- sequence after a few million years. After all the hydrogen is consumed at the cent re, the further evolution strongly depends on the mass of the star. For the purposes here, unless otherwise stated, we henceforth follow the evolution of low- mass stars ($\mathcal{M} \lesssim 2\mathcal{M}_\odot$).

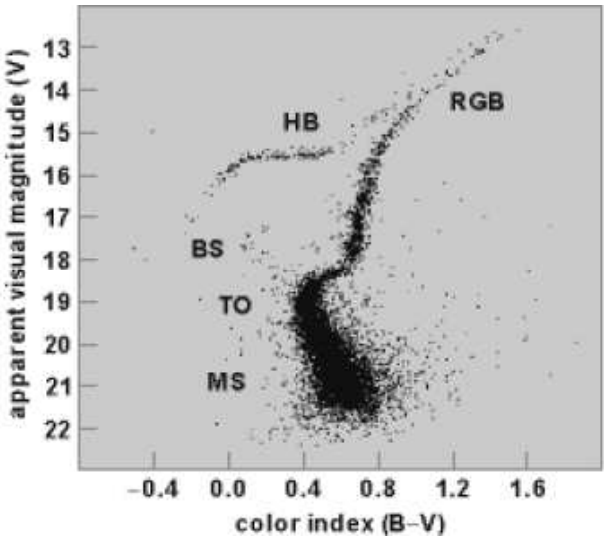

Figure 1.2: Colour- magnitude diagram with apparent visual magnitude (V) versus color index (B-V) for the globular cluster M3 according to Buonanno et al. (1986). The important evolutionary stages are marked by MS (main sequence), TO (turn-off), RGB (red giant branch), HB (horizontal branch), and BS (blue stragglers). Figure courtesy of http://www.accessscience.com

Red giants

After central hydrogen is consumed the star will have a core of helium surrounded by a thin hydrogen burning shell. With no outward pressure from the nuclear reactions to counteract gravity, the core contracts and becomes hotter. The heat from the contracting core increases the hydrogen burning in the shell above causing the layers in the outer envelope to expand. This decreases the gravitational pull of the core on the layers and they expand faster than the increased nuclear burning which causes them to cool. As the star becomes cooler, it becomes *redder*, and ultimately a *red giant*.

As hydrogen burning continues in the shell, helium is deposited onto the core which supports itself by thermal pressure. Soon it becomes so dense however, that the electrons become degenerate. Due to the inverse relationship between mass and radius in eq. 1.5, increasing the core mass makes the radius of the core smaller! The growing core mass causes the outer shell of the star to become even hotter. With the steep temperature dependence of the hydrogen burning rates, its luminosity increases. The star travels along the *red giant branch* (RGB) upwards (increasing luminosity) and to the right (lower surface temperature) on the Hertzsprung Russel diagram.

Helium ignition

The core of the red giant reaches its limiting mass when it has become so hot and dense that helium ignites. Helium is converted to carbon through the *triple- α reaction*[6], via an intermediate state of the unstable ^{8}Be state. The triple- α is a very temperature sensitive process and its energy generation rate per unit mass, $\epsilon_{3\alpha}$, scales approximately as $\sim \rho^2 T^{40}$! So when the temperature reaches the critical one high enough for onset of the triple- α reaction, there is a runaway nuclear reaction.

Due to the degenerate nature of the star, the energy production does change the structure at first. Therefore the rise in temperature goes only to feed the energy generation, which increases the nuclear reaction rate even more. As this continues, the core expands very quickly and finally becomes nondegenerate so that the usual self- regulation explained earlier kicks in.

Horizontal branch stars

The final configuration of a helium burning core and a hydrogen burning shell is known as horizontal- branch (HB) star. The name refers to the location of the star on the colour- magnitude diagram[7] of figure 1.2. (explain figure somewhere) Because of the expansion of the core, the gravitational potential at its boundary is lowered and thus so is the temperature in the hydrogen burning shell. Overall, the result that the luminosity has decreased by the process of helium ignition. The decrease in luminosity together with a contraction of the envelope with the following increase in surface temperature is what makes the star descend down to the HB from the RGB.

On the HB star evolves quietly at an almost constant luminosity, burning helium into carbon (^{12}C) and some of the carbon goes on to form oxygen (^{16}O). At the end of the horizontal branch the star has developed a degenerate core of carbon and oxygen with helium shell burning and continuing hydrogen shell burning.

White dwarfs

What happens when all the helium in the core is consumed is very similar to when the star which first ascends the RGB: it travels upwards and to the right in the HR diagram, asymptotically approaching the track of the first ascend. This

[6] The triple- α reaction goes as $3\alpha \rightarrow^{12} C$

[7] Colour- magnitude diagram is a type of HR diagram where the colour index of the UBV photometric system are used on the axis. The colour indices give the luminosity of the star in different filters.

is known as the *asymptotic giant branch* (AGB).

In low mass stars the carbon and oxygen never ignite. On the AGB the star experiences great mass- loss from the envelope. The remaining core becomes continues to radiate heat from its interior. As these stars are geometrically small (radius of $\sim 10^4 km$), their small surface area restricts their luminosity in spite of the great energy production, thereby the name *white dwarfs*. Since supported by degeneracy pressure, they cool by neutrino emission from the interior and photon emission from the surface until disappearing from visibility.

Supernova explosions and neutron stars

Massive stars ($\mathcal{M} \gtrsim 6 - 8\mathcal{M}_\odot$) evolve differently from the low- mass stars considered so far. Even after great mass- loss during the AGB, their cores reach high enough temperatures to ignite carbon and oxygen. When massive stars run out of fuel, and the core mass exceeds the Chandrasekhar limit (see the paragraph on degeneracy in section 1.1.1), they will no longer be supported by degeneracy pressure. This happens at temperatures and densities of $T \sim 10^{10} K = 0.7\,\mathrm{MeV}$ and $\rho \sim 3 \times 10^9 g\,cm^3$. The result is a core contraction leading to a type II *supernova explosion* with the release of tremendous amounts of energy, the main output being a burst of neutrinos. The core collapses to nuclear densities ($\sim 3 \times 10^{14}$) and forms a neutron star.

Globular- cluster stars

Globular clusters are gravitationally bound ensambles of typically 10^6 stars which form an almost spherical halo. What makes the globular clusters so interesting to study is the fact that the stars are formed at approximately the same time. Therefore they have very similar chemical composition; they differ only by their mass. In a colour- magnitude diagram of a globular cluster the stars arrange themselves in a characteristic pattern as in figure 1.2, the branches corresponding to the different phases of the stellar evolution. Since all the stars start at the main sequence at the same time, the colour- magnitude diagram represents an *isochrone* of a stellar population. There are almost no stars on the upper main sequence because the more massive stars have evolved faster and already left to become red giants. There is a distinct *turnoff* (TO) where the main sequence again is full of stars, below which the stars have not had time to finish hydrogen burning. Therefore, the stellar mass corresponding to the MS turnoff is a precise measure of the cluster age.

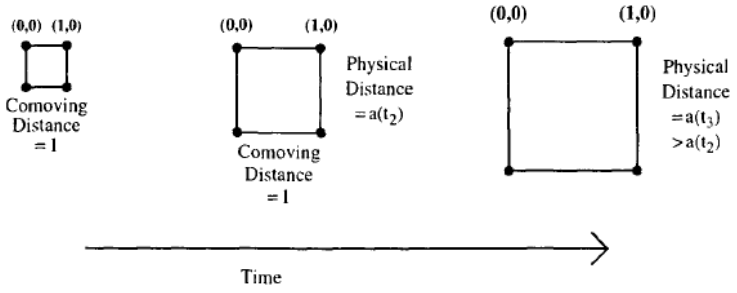

Figure 1.3: Expansion of the universe. The comoving distance between points on a hypothetical grid remains constant as the universe expands. Figure taken from[4]

1.2 General Relativity

The strongest force of nature on large scales is gravity, so the most important part of describing the universe is a theory of gravity. As far as we are presently aware, Einstein's theory of general relativity, published in 1916, gives an excellent description of gravitational physics. General relativity (GR) is thus a natural mathematical framework for the study of cosmology/cosmological models. Einstein's GR led cosmologists to the understanding of gravity not being a force. Rather it is a consequence of matter in the universe bending the spacetime surrounding it, warping its properties.

1.2.1 The tensor metric and the line element

General relativity implies that gravitation can be described by a *metric*. The metric is represented by a four- dimensional tensor, $g_{\mu\nu}$, which is used to define distances between neighboring points, x^μ and $x^\mu + dx^\mu$. Figure 1.3 shows that even if one knows the components of a vector in a coordinate system, additional information is needed in order to find the physical distance between the two vector components. The metric relates the coordinate distance to the physical distance. We are interested in the separation between points in four- dimensional spacetime, and we need to allow for the possibility that spacetime might be curved. Generally, this is given by the so called line element,ds, as

$$ds^2 = \sum_{\mu,\nu} g_{\mu\nu}\, dx^\mu\, dx^\nu. \tag{1.6}$$

Here dx^μ is the infinitesimal distance between two spacetime events. The indices μ and ν range from 0 to 3, where 0 represents the time-like component and the three others the space-like components. To relate the metric to the matter and energy in the universe, Einstein postulated a set of field equations.

1.2.2 Einstein equations

Einstein's field equations in their simplest form are

$$G_{\mu\nu} = 8\pi G\, T_{\mu\nu}, \tag{1.7}$$

where G is Newton's gravitational constant. The tensor $G_{\mu\nu}$ is called the Einstein tensor and is given by

$$G_{\mu\nu} \equiv R_{\mu\nu} - \frac{1}{2}\, g_{\mu\nu}\, \mathcal{R}.$$

Here $R_{\mu\nu}$ and $\mathcal{R}$ are the Ricci tensor and scalar respectively, where the latter is just a contraction of the Ricci tensor:

$$\mathcal{R} \equiv g_{\mu\nu}\, R_{\mu\nu}. \tag{1.8}$$

The Ricci tensor and scalar give the curvature of spacetime while the Einstein tensor represents the geometry. The tensor $T_{\mu\nu}$ is the energy-momentum tensor and its form depends on the type of energy present in the universe. We will only concider the constituents of the universe to be so called perfect fluids, i.e. a fluid with no viscosity nor heat flow ([5], page 151). Perfect fluids have energy-momentum tensor

$$T^{\mu}_{\nu} = diag\{-\rho c^2, p, p, p\}, \tag{1.9}$$

where ρ is the mass density and p is the pressure.

The left-hand side of Einstein's field equation is a function of the metric, i.e. the curvature, while the right- hand side represents the matter and energy. Hence the Einstein equations tells us how the curvature of spacetime reacts to the presence of energy- momentum.

1.3 Cosmology

Cosmology is the study of the universe as a whole. The most important feature of our universe is described by the *Cosmological principle*, i.e., at large scales the universe is both homogeneous and isotropic. Homogeneity is the property of being identical everywhere in space, while isotropy is the property of looking the same in every direction. This implies that no place in the universe is special which means that the same physical laws apply throughout the universe. For most of the twentieth century this was was taken as an assumption and remained an intelligent guess until firm data were finally obtained at the end of the twentieth century. (this is from Mukhanov p.3, CMB?)

1.3.1 The Friedmann- Robertson- Walker metric

Our current understanding of the evolution of the Universe is based upon the Friedmann-Robertson- Walker (FRW) cosmological model, usually called the hot big bang model. With the requirement of homogeneity and isotropy from the Cosmological principle the metric tensor becomes the FRW metric

$$g_{\mu\nu} = \begin{pmatrix} -1 & 0 & 0 & 0 \\ 0 & a^2(t) & 0 & 0 \\ 0 & 0 & a^2(t) & 0 \\ 0 & 0 & 0 & a^2(t) \end{pmatrix}, \tag{1.10}$$

where $a(t)$ is the scale factor describing the expansion of the universe. The first item on the diagonal is the time component and the other three are the space components. The line element for this metric is

$$ds^2 = c^2dt^2 - a^2(t)\left(\frac{dr^2}{1-k\,r^2} + r^2\,d\theta^2 + r^2 sin^2\theta\,d\phi^2\right), \tag{1.11}$$

where the spherical coordinates, r, θ and ϕ, are the comoving coordinates. The time parameter t is the *cosmic time* which is defined as the proper time of an observer who is at rest in the comoving coordinate system, i.e. is moving with the expansion of the universe. The curvature parameter, k, is a constant describing the geometry of the universe. For $k = +1$ the universe is said to be closed (but without boundaries) and has the geometry of a three-dimensional sphere. The scale factor $a(t)$ may, in this case, be interpreted as the 'radius' of the universe at time t. If $k = 0$, the geometry of space is the well-known Euclidean and we say that the universe is flat. And finally, for $k = -1$ the universe is said to be open with hyperbolic geometry.

1.3.2 The Friedmann equations

The FRW metric can be used to compute different properties of the universe, f.ex. distances and luminosities. For the metric to be completely determined we need

to know the behavior of the scale factor. How the scale factor evolves with time depends on the energy content of the universe and is given by the Friedmann equations. These comes from solving the Einstein equations, substituting for the FRW metric (eq. 1.10) and the energy-momentum tensor (eq. 1.9) and are

$$H^2 \equiv \left(\frac{\dot{a}}{a}\right)^2 = \frac{8\pi G}{3}\rho - \frac{kc^2}{a^2}, \tag{1.12}$$

$$\frac{\ddot{a}}{a} = -\frac{4\pi G}{3}\left(\rho + \frac{3p}{c^2}\right). \tag{1.13}$$

Here ρ is the total energy density of the perfect fluid. In the case of several fluids (i.e. several contributions to the energy density), ρ must include all contributions. The same goes for the total pressure p of the fluid. The dots imply derivatives with respect to cosmic time and the parameter $H = \dot{a}/a$ is the famous Hubble parameter, which is a measure of the expansion of the universe. The second Friedmann equation (1.13) is also called the acceleration equation since it describes the acceleration of the scale factor. If the fluids contribute to the total pressure, it further decelerates the expansion.

It is convenient to write the Friedmann equations in terms of the density parameters as

$$\sum_i = \Omega_i + \Omega_k = 1, \tag{1.14}$$

where $\Omega_i = \rho_i/\rho_c$ is the density parameter for the fluid i and ρ_C is the critical density,

$$\rho_C = \frac{3H^2}{8\pi G}, \tag{1.15}$$

i.e. the density needed to make the spatial geometry of the universe flat. The *curvature density parameter*, $\Omega_k = -k\,c^2/(a\,H)$, must be zero for the universe to be flat. With the present Hubble parameter expressed as $H_0 = 100\,h\,km\,s^{-1}\,Mpc^{-1}$, where h is the dimensionless Hubble parameter, the critical density today becomes

$$\rho_{crit} = 1.879 \times 10^{-29}\,h^2 g\,cm^{-3}. \tag{1.16}$$

The cosmological constant

When formulating GR, Einstein introduced the cosmological constant,Λ, because he believed the universe was static. The idea was to balance curvature, ρ and Λ to get $H(t) = 0$ and hence a static universe. The introduction of such a term is permitted by GR and nowadays the cosmological constant is considered

as a contribution to the energy density and pressure of the universe. Λ appears as an extra term in the Friedmann equations, so that

$$H^2 = \frac{8\pi G}{3}\rho - \frac{kc^2}{a^2} + \frac{\Lambda}{3}, \tag{1.17}$$

$$\frac{\ddot{a}}{a} = -\frac{4\pi G}{3}\left(\rho + \frac{3p}{c^2}\right) + \frac{\Lambda}{3}. \tag{1.18}$$

The effect of Λ is best seen from the acceleration equation. A positive cosmological constant gives a positive contribution to $\ddot{a}$, hence acting as a repulsive force. The cosmological constant can also be described as if it were a perfect fluid with energy density ρ_Λ and pressure p_Λ. If we write the Friedmann equations with this point of view and compare it to eq. 1.17, we see that $\rho_\Lambda = \Lambda/(8\pi G)$. With this energy density we obtain the following pressure for Λ

$$p_\Lambda = -\rho_\Lambda c^2. \tag{1.19}$$

Hence, for a positive cosmological constant, there is negative pressure. This means that as the universe expands, work is done on the Λ- fluid and this permits its energy density to remain constant even though the volume of the Universe is increasing. Concerning its physical interpretation, Λ is thought of as the *vacuum energy*, i.e. the energy that exists space when devoid of matter.

1.3.3 Evolution of the energy density

The continuity equation, describing the evolution of the energy density, is obtained from conservation of the energy- momentum tensor, $T^{\mu}_{\nu;\mu} = 0$,[8]

$$\dot{\rho} = -3\frac{\dot{a}}{a}\left(\rho + \frac{p}{c^2}\right). \tag{1.20}$$

This equation maintains energy conservation for the perfect fluid as the universe expands adiabatically. For a fluid with an equation of state

$$p = \omega\,\rho c^2, \tag{1.21}$$

where ω is a constant which is unique for each type of fluid, the continuity equation has the following solution

$$\rho = \rho_0\left(\frac{a_0}{a}\right)^{3(1+\omega)}. \tag{1.22}$$

Non- relativistic matter, also called *dust* has an equation of state $\omega = 0$, which gives

[8]The semicolon represents a co variant derivative and a summation over repeated μ index is assumed (Einstein summation convention). See [4],page 37, for more details

$$\rho_m = \rho_{m0} \left(\frac{a_0}{a}\right)^3. \tag{1.23}$$

For relativistic matter (radiation), $\omega = 1/3$, which gives

$$\rho_r = \rho_{r0} \left(\frac{a_0}{a}\right)^4. \tag{1.24}$$

The equation of state for the cosmological constant, eq. 1.19, shows that $\omega = -1$, hence confirming what we already know: The energy density for Λ,

$$\rho_\Lambda = \rho_{\Lambda 0} = \frac{\Lambda}{8\pi G}, \tag{1.25}$$

is constant of the evolution of the scale factor with time.

1.3.4 The ΛCDM model

The ΛCDM (abbreviation for: Lambda- cold dark matter) model is called the 'Standard model of cosmology' since it is currently the model which is in best agreement with observations. In this model the universe is dominated by dust (mostly in the form of cold dark matter, abbreviated CDM) and a positive cosmological constant. The observations seem to prefer a flat model ($k = 0$) with density parameters $\Omega_{m0} \approx 0.3$ and $\Omega_{\Lambda 0} = 1 - \Omega_{m0} \approx 0.7$. More specific values are attained from measurements of the cosmic microwave background (CMB). Recent best fit values from the seven-year WMAP analysis, from Larson et al. (2011) in ref. [6], are (the $_0$ subscript indicate that these are the values of today):

Ω_{b0}	=	0.0449 ± 0.0028
Ω_{c0}	=	0.222 ± 0.026
$\Omega_{\Lambda 0}$	=	0.734 ± 0.029
Ω_{m0}	=	0.266 ± 0.029
t_0	=	13.75 ± 0.13 Gyr
H_0	=	71.0 ± 2.5 km s^{-1} Mpc^{-1}
$\Omega_{c0}\, h^2$	=	0.1109 ± 0.0056

Here Ω_{b0} is the density parameter of baryonic matter, Ω_{c0} is that of cold dark matter and $\Omega_{\Lambda 0}$ that of dark energy. The age of the Universe is denoted t_0 and H_0 is the present Hubble parameter.

According to this model the energy density of the universe is presently dominated by *dark energy*. The standard explanation of dark energy is the cosmological constant. Another possibility, known as *quintessence*, are scalar fields whose energy density can vary in time and space.

Note that only 4% of the 26% making up the total matter content of the universe

is ordinary baryonic matter (protons, neutrons, electrons [9]). The remaining 22% are made up of so called *cold dark matter*, which will be further explored later in this thesis.

The Friedmann equations (1.17) and (1.18) for this model are

$$H^2 = \frac{8\pi G}{3}\left(\rho_m + \rho_\Lambda\right) \tag{1.26}$$

$$\frac{\ddot{a}}{a} = -\frac{4\pi G}{3}\left(\rho_m - 2\rho_\Lambda\right). \tag{1.27}$$

In this text we will, unless otherwise stated, do all the calculations with the assumption of this model being the one describing our universe.

1.3.5 A brief thermal history

From the cosmological principle we know that the universe expands adiabatically. And as observations today strongly indicate that the universe is expanding, this immediately leads us to expect the early universe to be very hot and dense. The picture of a universe evolving from this hot and dense state, namely the *hot Big Bang*, is incorporated in the ΛCDM model. What follows is a very brief overview over the different stages of the thermal evolution of the universe. For a more extensive view see, e.g. (Coles and Lucchin, [7]) which in addition to Elgarøy,[8] and Liddle, [9] were good references to this section.

Planck era

Before the so called Planck time, $t = 10^{-43}\,s$ after the Big Bang, known physics break down. What happens up until then can possibly be explained by *quantum gravity*.

Inflation

A very short time after the Big Bang, at about $t \approx 10^{-35}\,s$, the universe went through an extremely rapid expansion. At that time, the energy density of the universe must have been dominated by scalar fields contributing negative pressure. Inflation solves many problems in the Big Bang cosmology, such as the *horizon problem* and the *flatness problem* [10]. Also, inflation prepares for the large scale structures seen in the universe today. This happens since initial quantum

[9] Cosmologists tend to include electrons in baryonic matter (to the annoyance of particle physicists) even though this is technically incorrect (electrons are leptons).

[10] The horizon problem refers to the fact that different regions of the Universe share the same properties, such as temperature, without ever having been *causally* connected. The flatness problem is the curiosity that the density parameter, out of all the possible values it could have had, is so close to unity.

fluctuations are blown up by the expansion,thus creating perturbations in the smooth background.

Radiation domination

Today there is significantly more energy in nonrelativistic matter than radiation. However, since the energy density of radiation scales as a^{-4}, see eq. 1.24, while that of matter as a^{-3}, eq. 1.23, the very early universe must have been radiation dominated. After inflation ceases the universe is quite cold and dominated by non-relativistic particles. Then there is a period called *reheating* in which the energy of the inflation field decays into relativistic particles. The temperature then is so high that the photons and other relativistic particles constitute a single fluid.
(Particle physics perspective: After the inflation ends the universe is filled with a quark-gluon plasma. The quark- hadron transition, i.e. when free quarks and gluon's combine to baryons and mesons, occurs at about $t \approx 10^{-5}\, s$ after the Big Bang ($T \approx 200\, MeV$).
A few minutes into the expansion, the temperature has decreased sufficiently for neutrons and protons to combine to form nuclei, a process known as *nucleosynthesis*. The photons continues to interact with nuclei and free electrons.

Dust domination

The time when the energy density of the universe went from being dominated by radiation to being dominated by matter, called *matter-radiation equality*, happens at $t_{eq} \approx 10^4\, yr$. Eventually, after approximately $380\,000\, yr$, the universe cools down so much that electrons can combine with nuclei to form atoms, an epoch called *recombination*. This naturally leads to a rapid decrease in the electron abundance, and since the photons at this time only couple to electrons, they decouple from the matter. This process is known as *decoupling* and allowed the photons to travel unimpeded for the remainder of the universe's evolution (with exception of the occasional encounter with matter) thereby also creating the cosmic microwave background (CMB) observed by cosmologists today.

In the time following recombination the first structures in the universe started to form. Structure formation eventually leads to *reionization* when objects formed by gravitational collapse starts emitting energy capable of ionizing the neutral hydrogen. Electrons are again free to interact with free photons. Photons may be scattered, but scattering interactions are infrequent since the energy densities of both electrons and photons have decreased due to the expansion of the universe.

1.3.6 Statistical physics

We need to know some statistical properties of a gas in thermal equilibrium. The key quantity needed is the distribution function $f_i(\mathbf{p})$. This function tells us what fraction of the particles is in a state with momentum $\mathbf{p}$ at a given temperature T and is given by

$$f_i(\mathbf{p}) = \frac{1}{e^{(E_i(p)-\mu_i)/(k_B)} \pm 1} \tag{1.28}$$

Here k_B is the Boltzmann's constant, μ_i is the chemical potential of the species and the energy is $E_i = \sqrt{\mathbf{p}^2c^2 + m_i^2c^4}$ (m_i is the rest mass of a particle species i). The plus sign is for fermions and the minus for bosons. Once the distribution function is given one can easily compute the equilibrium properties of the gas such as number density, energy density and pressure, respectively:

$$n_i = \frac{g_i}{(2\pi\hbar)^3} \int f_i(p)\, d^3p \tag{1.29}$$

$$\rho_i\, c^2 = \frac{g_i}{(2\pi\hbar)^3} \int E_i(p)\, f_i(p)\, d^3p \tag{1.30}$$

$$P_i = \frac{g_i}{(2\pi\hbar)^3} \int \frac{p^2}{3\, E(p)}\, f_i(p)\, d^3p. \tag{1.31}$$

The quantity g_i is the number of internal degrees of freedom of the particle which is related to the degeneracy of a momentum state. When computing the quantities of equations (1.29)- (1.31), we will normally be interested in either the non-relativistic limit, corresponding to $m_i\, c^2/k_B \gg 1$ or the ultrarelativistic limit, corresponding to $m_i\, c^2/k_B \ll 1$. Rewriting the integrals above as integrals over the particle energy E_i instead of the momentum p, and solving them for the the non- relativistic limit; the number density, energy density and pressure become

$$n_i = g_i \left(\frac{m_i k_B T}{2\pi\hbar^2}\right)^{(3/2)} exp\left(\frac{\mu_i - m_I^2}{k_B}\right) \tag{1.32}$$

$$\rho_i\, c^2 = n_i\, m_i\, c^2 \tag{1.33}$$

$$P_i = n_i\, k_B T, \tag{1.34}$$

respectively. These results for the non-relativistic limit are independent of whether the particles are fermions or bosons, i.e. whether they obey the Pauli exclusion principle or not. In the ultrarelativistic limit however, the results differ for fermions and bosons. Therefore we will state the result for the general case where the quantities get contributions from both non- relativistic and relativistic particles. The energy density and pressure of non-relativistic particles

is exponentially suppressed compared to ultrarelativistic particles. In the early universe (up to matter-radiation equality) it is therefore a good approximation to include only the contributions from ultrarelativistic particles in the sums. With this approximation, the general expression for the energy density is

$$\rho c^2 \approx \frac{\pi^2}{30}\frac{(k_B T)^4}{(\hbar c)^3}\left[\sum_{i=bosons} g_i\left(\frac{T_i}{T}\right) + \frac{7}{8}\sum_{i=fermions} g_i\left(\frac{T_i}{T}\right)\right],$$

where we have defined the effective number of relativistic degrees of freedom as

$$g_* = \left[\sum_{i=bosons} g_i\left(\frac{T_i}{T}\right) + \frac{7}{8}\sum_{i=fermions} g_i\left(\frac{T_i}{T}\right)\right]. \tag{1.35}$$

With this definition the energy density becomes

$$\rho c^2 = \frac{\pi^2}{30} g_* \frac{(k_B T)^4}{(\hbar c)^3}. \tag{1.36}$$

We now take a closer look at the parameter g_*.

Effective number of relativistic degrees of freedom

The effective number of relativistic degrees of freedom g_* depends on how many particles are ultrarelativistic, their internal degrees of freedom and their temperature, T_i, relative to the photon temperature, T. Note that the temperature dependency often is weak. The factor of 7/8 accounts for the difference in Fermi and Bose- Einstein statistics. We will now determine g_* for some temperatures by looking at the contributions of degrees of freedom from all particle species that are relativistic at T.

In the low temperature limit, when $T \ll$ MeV, g_* only receives contributions from the three relativistic neutrino species and the photon. Each neutrino contributes 7/4 degrees of freedom and the photon contributes $g_\gamma = 2$. The function then takes on the number $g_* \approx 3.36$, [10]. This is also the present number for g_*.

At temperatures of order 1 MeV, the contributing species are: photons ($g_\gamma = 2$), neutrinos ($g_\nu = 6$) and electrons and positrons ($g_{e^+} = g_{e^-} = 2$). Adding these up leads to $g_* = 10.75$, see ref. [4]. At higher temperatures, but still below so called colour confinement (quark- hadron transition, explained in section..), there are also contributions from pions and by the low-energy tails of the heavier mesons and baryons.

When the colour confinement occurs at T_{QCD}, the hadron contributions are replaced by contributions from quarks, gluon's and the Higgs boson[11], [10]. This

[11]The Higgs boson is a hypothetical, massive particle predicted by the SM.

causes a fast increase of g_* to about 100 for $T \gg T_{QCD}$. More specifically, for $T \gtrsim 300\,\text{GeV}$, all the species of the Standard Model should be relativistic leading to a value of $g_* = 106.75$, ref. [11].

Entropy density

The entropy is a function of volume V and the temperature T as

$$S = \frac{a^3\,(\rho\,c^2 + P)}{T},$$

where we have taken $V = a^3$. The equation for energy conservation states that $d[(\rho\,c^2 + p)\,V] = V\,dP$ so that $dS = 0$, which means that the entropy per comoving volume is conserved. Entropy density is defined as

$$s = \frac{S}{V} = \frac{(\rho\,c^2 + p)}{T}. \tag{1.37}$$

Substituting the energy density in eq. 1.36 with the pressure given by $P = \frac{1}{3}\,\rho\,c^2$ into equation 1.38 , the entropy density can be written as

$$s = \frac{2\pi^2}{45}\,k_B\,g_{*s}\left(\frac{k_B T}{\hbar\,c}\right)^3. \tag{1.38}$$

where we have introduced a new effective number of degrees of freedom for entropy density

$$g_{*s} = \left[\sum_{i=bosons} g_i\left(\frac{T_i}{T}\right) + \frac{7}{8}\sum_{i=fermions} g_i\left(\frac{T_i}{T}\right)\right]. \tag{1.39}$$

In general, $g_{*s} \neq g_{*s}$, but in the early universe the difference is small. The constancy of S implies that $s\,a^3 =$ constant, so from 1.38 we conclude that

$$s = g_{*s}\,T^3\,a^3 = \text{constant}. \tag{1.40}$$

1.3.7 The Boltzmann equation

The Boltzmann equation formalizes the statement that the rate of change of the abundance of a particle species is equal to the rate at which it is produced minus the rate at which it is annihilated. Suppose we are interested in how the number density of a particle species 1, n_1, changes with time in the expanding universe. Furthermore, let us assume the only process changing the particle's abundance is the annihilation with a particle 2, producing two new particles, 3 and 4 in the process $1 + 2 \longrightarrow 3 + 4$. The reverse process is also taking place, and in equilibrium the two processes are in balance. The ordinary differential equation describing this process is the Boltzmann equation, ref. [4]:

$$a^{-3}\,\frac{d(n_1\,a^3)}{dt} = n_l^{(0)} n_2^{(0)}\,\langle\sigma_A v\rangle\left[\frac{n_3 n_4}{n_3^{(0)} n_4^{(0)}} - \frac{n_1 n_2}{n_1^{(0)} n_2^{(0)}}\right], \tag{1.41}$$

where $n_i^{(0)}$ denotes the number density of species i in thermal equilibrium at temperature T, σ_A is the annihilation cross section, where we have summed over all the possible leptons l, and v is the relative velocity. The *thermally averaged* product of the latter two, $\langle\sigma_A v\rangle$, measures the reaction rate in the medium.

1.4 Quantum Field Theory

Quantum field theory is a theoretical framework that combines quantum mechanics and special relativity. The foundation of a systematic quantum theory of fields were laid by Dirac in 1927 in his famous paper on "The Quantum Theory of the Emission and Absorption of Radiation". From the quantization of the electromagnetic field one is naturally led to the quantization of any classical field. The quanta of the field are particles with well-defined properties. The interactions of these fields are mediated by other fields whose quanta are other particles.

In this section we will first review the Lagrangian formalism and apply it to classical field theory. Then we will utilize canonical formalism which provides a systematic quantization procedure for any classical field theory derivable from a Lagrangian. Note that the following theory is developed under the assumption of flat spacetime.

1.4.1 The Lagrangian formalism

In classical mechanics the Lagrangian formalism is an alternative method to Newtonian mechanics that can be used to derive the equations of motion of a system. The latter are found from *Hamilton's principle*, also known as the *Principle of least action*. The principle is formulated by the use of an *action integral*,

$$S = \int_{t_1}^{t_2} L\,(q, \dot{q}, t)\,dt,$$

the time integral from a time t_1 to a time t_2 of a function L called the *Lagrangian*, defined as the kinetic energy T minus the potential energy V. The Lagrangian is a function of the degrees of freedom of the system, q_i, and their time derivatives $\dot{q}_i$, the variables that describe the position and velocity of the particles making up the system. In addition, the Lagrangian depends on time. Hamilton's principle states that the action should have a stationary value, e.g. $\delta S = 0$ for a small variation in the path, $q \longrightarrow \delta q$. This leads to the *Euler- Lagrange equations*

$$\frac{d}{dt}\frac{\partial L}{\partial \dot{q}_i} - \frac{\partial L}{\partial q_i} = 0, \tag{1.42}$$

which are valid for any physical system appropriately described by a Lagrangian.

Classical field theory

A field has a physical quantity designated to every point in spacetime. They are considered to be functions of time at every point in spacetime,$\boldsymbol{x}$ and can be classified as a scalar, vector or tensor- field according to whether the value of the

field at each point is a scalar, a vector or a tensor, respectively. The Lagrangian formalism can easily be extended from a discrete system with coordinates $q_i(t)$ to a system which requires several fields $\phi_i(\mathbf{x}, t)$, $i = 0, .., N$ to specify it. The index i may label components of the same field or it may refer to different independent fields. Because the action must be Lorentz invariant to satisfy the principle of relativity, the Lagrangian in field theory is replaced by the *Lagrangian density*, $\mathcal{L}$, defined via

$$L = \int \mathcal{L}\, d^3x.$$

The Lagrangian density is a function of the fields and their first derivatives $\mathcal{L} = \mathcal{L}(\phi_r, \phi_{r,\mu})$. Applying Hamilton's principle with an action $S = \int \mathcal{L}\, d^4x$, where d^4x is a four- dimensional element, one obtains the Euler- Lagrange equations for fields,

$$\frac{\partial \mathcal{L}}{\partial \dot{\phi}_r} - \frac{\partial}{\partial x^\mu}\left(\frac{\partial \mathcal{L}}{\partial \phi_{r,\mu}}\right) = 0, \qquad r = 1, ..., N. \tag{1.43}$$

Quantization

The process of quantization is based on imposing commutation relations. *Canonical quantization* refers to the process of promoting position and momentum functions to operators and imposing the commutation relations. When quantizing a classical field theory the fields are promoted to operators and commutation relations are imposed, a procedure known as *second quantization*. We will work in the Heisenberg picture, in which the state vectors are time- independent while the operators evolve in time.

We are dealing with a system with an infinite number of degrees of freedom, corresponding to the values of the fields ϕ_i. Approximating the system by one having a finite number of degrees of freedom, we decompose the three- dimensional space into small cells of equal volume, $\delta\mathbf{x_j}$. The system is now described by a set of generalized coordinates

$$q_{rj} \equiv \phi_r(j, t) \equiv \phi_r(\mathbf{x}_j, t), \quad j = 1, 2, ..., \quad r = 1, ..., N, \tag{1.44}$$

which are the values of the fields at the discrete lattice sites $\mathbf{x_j}$. Replacing the spatial derivatives of the fields by their difference coefficients between neighboring sites, we can write the Lagrangian of the discrete system as

$$L(t) = \sum_j \delta\mathbf{x}_j\, \mathcal{L}_j\left(\phi_r(j, t), \dot{\phi}_r(j, t), \phi_r(j', t)\right).$$

The parameter $\phi_r(j', t)$ is included because the Lagrangian density in the jth cell depends on the fields at the neighboring lattice sites j'.

We define the conjugate momentum to the coordinate q_i as

$$p_i = \frac{\partial L}{\partial \dot{q}_i},$$

which for q_{rj} becomes

$$p_{rj}(t) = \frac{\partial L}{\partial \dot{q}_{rj}} \equiv \frac{\partial L}{\dot{\phi}_r(j,t)} \equiv \frac{\partial \mathcal{L}_j}{\dot{\phi}_r(j,t)} \equiv \pi_r(j,t)\,\delta\mathbf{x_j}. \tag{1.45}$$

The canonical commutation relations for classical mechanics are given by

$$[\,\hat{q}_i, \hat{q}_j\,] = 0, \quad [\,\hat{p}_i, \hat{p}_j\,] = 0, \quad [\,\hat{q}_i, \hat{p}_j\,] = i\hbar\,\delta_{ij} \tag{1.46}$$

Here δ_{ij} is the Kronecker delta (should I state it?) We can now easily go from the classical to the quantum field theory by first interpreting the conjugate coordinates and momenta of the discrete lattice approximation, (1.44) and (1.45), as Heisenberg operators. Secondly, these will be subjected to the commutation relations (1.46). If we let the lattice spacing go to zero we arrive at the commutation relations for the fields:

$$\begin{aligned}
&[\,\phi_r(\mathbf{x}, t),\ \pi_s(\mathbf{x}', t)\,] = i\hbar\,\delta_{rs}\,\delta(\mathbf{x} - \mathbf{x}') \\
&[\,\phi_r(\mathbf{x}, t),\ \phi_s(\mathbf{x}', t)\,] = [\,\pi_r(\mathbf{x}, t), \pi_s(\mathbf{x}', t)\,] = 0,
\end{aligned} \tag{1.47}$$

where $\delta(\mathbf{x} - \mathbf{x}')$ is the three- dimensional Dirac delta function. Note that (1.47) are *equal- time commutation relations*, i.e. the fields are evaluated at equal times.

1.4.2 Symmetries and conservation laws

It follows from Heisenberg's equation of motion of an operator $O(t)$,

$$i\hbar\,\frac{dO(t)}{dt} = [\,O(t),\, H\,],$$

that O is a constant of motion provided that $[O, H] = 0$. For a field theory derived from a Lagrangian density $\mathcal{L}$, it can be shown that invariance of $\mathcal{L}$ leads to equations of the form

$$\frac{\partial f^\mu}{\partial x^\mu} = 0, \tag{1.48}$$

where f^μ are functions of the field operators and their derivatives. Defining

$$F^{\alpha}(t) = \int f^{\alpha}(\mathbf{x}, t)\, d^3\mathbf{x},$$

then equation 1.48 gives

$$\frac{1}{c}\frac{dF^0(t)}{dt} = -\int \sum_{j=1}^{3} \frac{\partial}{\partial x^j} f^j(\mathbf{x}, t)\, d^3\mathbf{x} = 0,$$

where the last equality follows from using Gauss' divergence theorem and assuming that the fields, and hence f^j, tend to zero at infinity. Or alternatively, if one uses a finite normalization volume with periodic boundary conditions, the surface integral vanishes. Now

$$F^0(t) = \int f^0(\mathbf{x}, t)\, d^3\mathbf{x} = 0$$

is a conserved quantity. To sum up; the invariance of the Lagrangian density, $\mathcal{L}$, under a continuous symmetry transformation implies a conserved quantity. This is known as *Noether's theorem*. Invariance of $\mathcal{L}$ under spacetime translations yields conservation of energy or linear momentum while invariance under rotations yields conservation of angular momentum.

1.4.3 The Klein Gordon equation

The Klein Gordon equation is a relativistic version of the Schrdinger equation. For particles of rest mass, m, energy and momentum are related by

$$E^2 = m^2c^4 + c^2\mathbf{p}^2.$$

It particles can be described by a single scalar wavefunction $\phi(x)$, the prescription of non-relativistic quantum mechanics

$$\mathbf{p} \longrightarrow i\hbar\nabla, \quad E \longrightarrow i\hbar\,\tfrac{\partial}{\partial t},$$

results in a relativistic wave- equation

$$\frac{1}{c^2}\frac{\partial^2\phi}{\partial t^2} - \nabla^2\phi - \frac{m^2c^2}{\hbar^2} = 0, \tag{1.49}$$

known as the *Klein- Gordon equation*. Written more compactly on co variant form, with natural units

$$(\Box + \mu^2)\,\phi(x) = 0, \tag{1.50}$$

where $\mu = m\,c/\hbar$. The operator $\Box$ is a scalar known as the D'Alembertian operator and is defined by

$$\partial^{\alpha}\partial_{\alpha} = \frac{1}{c^2}\frac{\partial^2}{\partial t^2} - \nabla^2 \equiv \Box. \tag{1.51}$$

This equation can also be obtained by substituting the Lagrangian density,

$$\mathcal{L} = \frac{1}{2}\left(\phi_{,\alpha}\,\phi^{\alpha}_{,} - m^2\phi^2\right), \tag{1.52}$$

for a single real field, $\phi(x)$ into the Euler- Lagrange equations, eq. 1.43. The Klein- Gordon equations are the equations of motions of a relativistic scalar field described by the Lagrangian in 1.52.

1.5 Particle physics

The main application of quantum field theory is to the study of particle physics. The aim of particle physics is describing the elementary sub-atomic particles and the interactions between them by means of the *Standard model*.

1.5.1 The Standard Model

The Standard Model (SM) is a highly successful model describing the properties of the fundamental particles and interactions between them. It was developed early and in the middle of the 20th century and the current formulation was finalized in the 1970's with the experimental confirmation of the existence of quarks. The SM can be summarized this way:

> *All the known matter in the universe is made up of quarks and leptons, held together by fundamental forces which are represented by the exchange of particles know as gauge bosons.*

Quarks

Quarks are fermions, i.e. particles of half- integer spin. They have fractional charge and combine to form composite particles called *hadrons*. Hadrons are divided into baryons and mesons, where the first consist of a combination of three quarks and the latter of two quarks (examples are protons, neutrons and pions). Each quarks has three internal degrees of freedom, a property known as colour.

Leptons

Leptons are also fermions with spin 1/2, but have integer charge. There are six types of leptons forming three generations. The three are electrons, muons and taus and they each with their corresponding neutrino.

1.5.2 Gauge theory

In the SM there are three types of gauge bosons (particles of integer spin), photons, W and Z bosons, and gluon's. Each corresponds to one of the three fundamental interactions described in the standard model, the *electromagnetic interaction*, the *weak interaction* and the *strong interaction*, respectively. For each of the interactions there is a gauge field and the gauge bosons are the quanta of that field. The number of gauge bosons that exist for a particular field is given by the number of *generators* of the field. Generators come from the unitary group used to describe the symmetries of the field. In a *gauge theory* the Lagrangian is invariant under local gauge transformations. The term *gauge* refers to the

degrees of freedom in the Lagrangian. These transformations form the unitary group associated with the gauge field.

As an example, let us consider the simplest unitary group U(1), represented by the unitary operator $U = e^{-i\theta}$, where θ is a real parameter. A U(1) symmetry implies that a Lagrangian $L = L(\phi, \partial_\mu \phi)$ is invariant under a gauge transformation

$$\phi(x) \rightarrow \phi'(x) = e^{-i\theta}\, \phi(x). \tag{1.53}$$

The field theory described by such a Lagrangian is a gauge theory with the U(1) symmetry group. When θ does not depend on the spacetime coordinate x, then we say that eq. 1.53 is a *global* gauge transformation. On the other hand, if $\theta = \theta(x)$, eq. 1.53 depends on location and we say that it represents a *local* gauge transformation.

The Standard Model is a *non- Abelian* (explained further ahead) gauge theory with the symmetry group $SU(3) \times SU(2) \times U(1)$.

1.5.3 Fundamental interactions

There are four fundamental interactions. The first three are, as already mentioned, described by the standard model while the fourth, gravity is not.

The electromagnetic interactions

The electromagnetic interactions are described classically by Maxwell's equations and in the quantum regime by quantum field theory known as *quantum electrodynamics* (QED). These forces are mediated by a well known massless gauge boson, the photon. The coupling constant which measures the strength of the interactions is $g_{EM} \sim e$, the elementary charge. Often it is replaced by the *fine structure constant*,

$$\alpha = \frac{e^2}{\epsilon_0 \hbar c} \simeq 1/137. \tag{1.54}$$

QED is the gauge theory of electromagnetism. Its Lagrangian density, $\mathcal{L}_{QED}$ is invariant under the, already discussed, U(1) unitary group.

The weak interactions

The weak interactions involve all particles, but are generally of most interest when they involve leptons. They are caused by the exchange of W and Z bosons (called W^+, W^- and Z_0) and are thus of short range because these bosons

have mass. The electromagnetic and weak interactions are believed to have been unified in a single force called the elctroweak force. The electroweak force is, for energies greater than $f_{EW} \cong 250\,\text{GeV}$, described by a Lagrangian which is invariant under the group of gauge transformations denoted SU(2) × U(1). At energies lower than E_{EW} the symmetry given by the SU(2) × U(1) transformation group is spontaneously broken. The consequence of this is that the leptons (except perhaps the neutrinos) and the three bosons acquire masses.

The strong interactions

The strong interactions are needed to overrule the electromagnetic repulsion between quarks of the same charge, in order for them to bind into hadrons. In addition, they are needed to hold nucleons (protons and neutrons) together in nuclei, hence often referred to as the *strong nuclear force*. The carriers, i.e. the gauge bosons, of the strong interactions are the *gluon's*. Gluon's themselves possess colour charge and are thus able to interact directly with other gluon's. This possibility is not available in electrodynamics, as photons do not posses electric charge. Theories in which quanta may interact directly are called *non- Abelian*.

In analogy to the electromagnetic interactions, the quantum mechanical description of the strong interactions are given by a theory known as *Quantum Chromodynamics*, abbreviated QCD. QCD is a non- Abelian gauge theory based on the U(3) symmetry group.

Gravity

The gravitational interactions are described classically by general relativity. Gravity is special in that it affects all particles, and that it is normally negligible compared with the other forces in elementary particle processes. This is fortunate, since gravity is the only force for which we do not have a satisfactory quantum mechanical description.

Grand Unification?

There are different theories called GUT's (Grand Unified Theories) which attempt to unify the strong and electroweak interactions. The simplest version of a GUT respects the SU(5) symmetry group which is spontaneously broken at an energy of $E_{GUT} \cong 10^{15} GeV$, so that $SU(5) \rightarrow SU(3) \times SU(2) \times U(1)$.

1.5.4 Spontaneous symmetry breaking

To introduce the concept of *spontaneous symmetry breaking*, we will take a look at the Lagrangian

$$\mathcal{L} = \frac{1}{2}\left(\partial_\mu \phi\right)^2 + \frac{1}{2}\mu^2\phi^2 - \frac{\lambda}{4}\phi^4, \tag{1.55}$$

which is invariant under the transformation $\phi \to -\phi$. In some cases, a system that has some symmetry existing in the Lagrangian may have a ground state (i.e. vacuum state) that does not satisfy the same symmetry. Imagine a ball at rest on the top of a spherically symmetric hill, placed right at the cent re. From the point of view of the ball, every direction down to the ground level is equivalent, i.e. the system i symmetric. However, the system is unstable. A small perturbation and the ball starts rolling down in one direction. In the analogy with QFT, the ball sitting on top of the hill represents the unstable ground state. When the ball starts to roll down in one direction we say that the symmetry is spontaneously broken. The ball has now arrived at the state of minimal potential energy, i.e. the *true* ground state of minimal potential energy is when the symmetry is broken and the ball finds itself resting on the ground.

In QFT we often have lagrangians that exhibit similar properties to the ball sitting on top of the hill. There is an apparent ground state, but there will be a *true* ground state of lower energy that leads to symmetry breaking. Vacuum is the state with no fields, i.e. $\phi = 0$. In perturbation theory, we expand about $\phi = 0$ and the fields are then viewed as fluctuations about the ground state. Since the Lagrangian is defined as $L = T - V$, the state with $\phi = 0$ is not always the minimum. The true ground state is found by

$$\frac{\partial V}{\partial \phi} = 0.$$

For the Lagrangian in 1.55, the potential is $V(\phi) = -\frac{1}{2}\mu^2\phi^2 + \frac{\lambda}{4}\phi^4$, giving the following minimum

$$\phi = 0, \quad \phi = \pm\sqrt{\frac{m^2}{\lambda}}$$

The state case of $\phi = 0$ corresponds to the unstable point with the ball resting on the top of the hill. The two other values give true ground states. Choosing one or the other breaks the symmetry in analogy to the ball rolling down the hill coming to rest at a particular point on the ground. The Lagrangian is no longer invariant under $\phi \to -\phi$, but we will gain knowledge of the mass of the particle associated from the field. A mass term in the Lagrangian is one that is quadratic in the fields. For instance if the Lagrangian for a field ϕ includes a term $-\alpha^2\phi^2$,

then α is the mass of the particle associated with the field, provided that $\alpha^2 > 0$.

Phase transitions in cosmology

Symmetry- breaking phase transitions play an important role in cosmology. In the hot early universe the vacuum, i.e. the various quantum fields that fill the space, possessed a large number of symmetries. As the universe expanded and cooled, the vacuum underwent a series of symmetry- breaking phase transitions, as already explained for example in the section on the weak interactions above.

In the remainder of this thesis, we will mostly hear about the QCD phase transition which occurs at a temperature of $T_{QCD} \sim 200\,\text{MeV}$[12]. This transition is also called the *colour confinement* or the *quark- hadron transition*, since it represents the time when hadrons start forming from the quark-gluon soup.

[12]Various authors operate with different values for the temperature of the QCD phase transition, T_{QCD}. Wantz et. al., ref. [12], show in fig. 3 that it occurs at a temp of approx. 180 MeV. Raffelt uses $T_{QCD} \approx \Lambda_{QCD} \approx 200\,\text{MeV}$, see ref.[13]. An updated Raffelt article, ref. [14], operates with a temperature of $T_{QCD} \approx 150\,\text{MeV}$. Recent lattice data, ref. [15], suggests that the QCD phase transition is a cross-over rather than a sharp phasetransition

Chapter 2

The Axion

Quantum chromodynamics is almost universally believed to be the theory of the strong interactions, but it has one serious difficulty; the *Strong CP problem*. The axion is a prediction of the most elegant solution to this problem, namely the Peccei- Quinn theory. If axions exist they have important astrophysical and cosmological implications, providing closure density.

In this chapter the axion will be introduced through the strong CP problem and the Peccei- Quinn mechanism. The different axion models will be studied and we will look at how axions interact with fermions and photons. Helpful references for this chapter were *Stars as Laboratories for Fundamental Physics*, ref.[1], *Astrophysical methods to constrain axions and other novel particle phenomena*, ref. [13] and *The Early Universe*, ref. [11].

2.1 The Strong CP Problem

The electroweak and strong gauge interactions are invariant under CP transformations. CP is the product of two symmetry transformations; *charge conjugation* (C) and *parity transformation* (P). Invariance under charge conjugation implies that the laws of physics should be the same if each charge $\mathbf{q}$ were interchanged with $-\mathbf{q}$, hence interchanging particles with their antiparticles. Parity transformation involves a space inversion- a simultaneous flip in sign of all coordinates.

In addition to the usual colour gauge interactions, the Lagrangian describing QCD has the following term

$$\mathcal{L}_\theta = \overline{\theta}\,\frac{\alpha_s}{8\pi}\,G\tilde{G}, \tag{2.1}$$

where $\alpha_s \simeq g_s^2/4\pi$ is the fine structure constant of strong interactions with g_s the strong Yukawa coupling constant, more accurately given in ref. [16]. The product $G\tilde{G} = G_b^{\mu\nu}\tilde{G}_{b\mu\nu}$, where $G_b^{\mu\nu}$ is the colour field strength tensor and $\tilde{G}_{b\mu\nu} = \frac{1}{2}\epsilon_{\mu\nu\rho\sigma}G_b^{\rho\sigma}$

is its dual. The variable b implies a summation over the colour degrees of freedom and $\overline{\theta}$ is given by

$$\overline{\theta} = \theta + \arg\det M_q. \tag{2.2}$$

The parameter θ characterizes the QCD ground state, also called the "θ- vacuum". For the transformation $\theta \rightarrow \theta + 2\pi$ maps the θ- vacuum onto itself, meaning that the θ- vacuum for θ has the same value as the θ- vacuum for $\theta = \theta + 2\pi$. Different ground states are thus characterized by values in the range $0 \leq \theta \leq 2\pi$. See ref. [11] for further explanation of the vacuum state.

The second term in 2.2 is the phase of the *quark mass matrix*, M_q. The masses of quarks are thought to arise from their interaction with a scalar field, the so called *Higgs field* [1]. The result of this interaction is a complex quark mass matrix M_q. The M_q matrix can be made real and diagonal by a suitable transformation of the quark fields. This procedure leads to the term, $\arg\det M_q$, in the QCD Lagrangian due to the involvement of a global chiral phase transformation (the term *chiral* refers to which representation is used for the Dirac Matrices).

The Lagrangian in eq. 2.1 changes sign under a CP transformation, thus violating the CP invariance of QCD [2]. CP violation leads to a neutron electric dipole moment of the size $d_n \approx \mid \overline{\theta} \mid 10^{-16}\, e\, cm$ [3]. The present experimental bound to the electric dipole moment of the neutron is $d_n \lesssim 5 \times 10^{-25}\, e\, cm$, indicating that $\mid \overline{\theta} \mid \lesssim 10^{-9}$. Theoretically we expect the value of the free parameter $\mid \overline{\theta} \mid$ to be of order unity. The smallness of $\mid \overline{\theta} \mid$ is referred to as the strong CP problem.

Note that in the case of one or more quarks being massless, the $G\tilde{G}$- term would have no physical effects. The term $\det M_q$, and thereby also $\overline{\theta}$ would vanish, and there would be no CP problem. Since there does not seem to any massless quarks in our world though, we need to take a closer look at the most compelling solution to this problem.

2.2 Peccei- Quinn theory

The most elegant solution of the strong CP problem is the so called *Peccei- Quinn theory* (QP) proposed by Peccei and Quinn in 1977, ref. [18, 19]. The theory explains the experimentally observed smallness of the neutron electric dipole moment resulting from the CP violating term of the QCD- Lagrangian. The idea

[1] This is the *Higgs mechanism*, see e.g. ref. [17] for further explanation.

[2] The structure of the product of the colour field strength tensor with its dual is $G\tilde{G} \propto \mathbf{E}_{\mathbf{colour}} \cdot \mathbf{B}_{\mathbf{colour}}$, i.e. the scalar product of a polar with an axial vector and so is CP odd

[3] More precisely by $d_n \approx \mid \theta \mid (0.04 - 2.0) \times 10^{-15}\, e\, cm$, (Baluni 1979; Crewther et al. 1979 and Cheng 1988).

is to reinterpretate the parameter | $\overline{\theta}$ | as a physical field; the axion field, which assures that $\mathcal{L}_\theta$ vanishes dynamically. The axion field a(x) enters the QCD-Lagrangian (rewrite this sentence?)

$$\mathcal{L}_\theta = (\overline{\theta} - a/f_a)\,\frac{\alpha_s}{8\pi}\,G\tilde{G} \tag{2.3}$$

where f_a is the Peccei- Quinn scale, also called *axion decay constant*. The complete Lagrangian also contains a kinetic term for the axion field, but no potential term. The lack of a potential term implies that the axion is massless. With only a kinetic term, the Lagrangian will remain invariant (except for the interaction term 2.3) under a global shift $a(x) \longrightarrow a(x) + a_0$, where a_0 is a constant (remember that the kinetic term involves derivation, thus cancelling the constant a_0). Making this substitution into the interaction term we find that defining the constant, $a_0 = \overline{\theta} f_a$, leads $\overline{\theta}$ to vanish. This invariance of the rest of the Lagrangian thus allows $\overline{\theta}$ to be absorbed into the definition of the axion field by the given choice of a_0. The axion- Lagrangian, when including the kinetic term then becomes

$$\mathcal{L}_a = \frac{1}{2}(\partial_\mu a)^2 - \frac{\alpha_s}{8\pi f_a}\,a\,G\tilde{G}. \tag{2.4}$$

Since the $G\tilde{G}$- term is CP- odd the axion has to be CP- odd for this Lagrangian to be CP invariant. The axion being CP- odd means $a \rightarrow -a$ under a CP transformation which implies that the axion has negative parity. Particles of negative parity are called *pseudoscalars*. Thus by construction, axions are pseudoscalar particles, more specifically they are pseudoscalar bosons of spin zero. Other examples of pseudoscalars include neutral pions π and K mesons.

The $aG\tilde{G}$ coupling is a generic feature of axions and has an important implication which is the key feature of the PQ- theory: Although constructed to be massless, axions acquire an effective mass by their interactions with gluon's. In an effective low-energy theory, the axion- gluon interaction allows for transitions to $q\overline{q}$ states (states made up of one quark and one antiquark, for example the neutral pion π^0). See figure 2.2. Physically this means that axions and pions mix and thereby axions pick up a small mass approximately given by

$$m_a f_a \approx m_\pi f_\pi, \tag{2.5}$$

where $m_\pi = 135\,\text{MeV}$ is the pion mass and $f_\pi \approx 93\,\text{MeV}$ its decay constant.

The presence of this mass term implies that at low energies the axion Lagrangian contains a potential $V(a)$. To the lowest order the potential expands as $\frac{1}{2}m_a^2 a^2$. Even if one does not introduce axions there exists a vacuum energy density $V(\overline{\theta}) \sim \frac{1}{2}\,\overline{\theta^2}\,m_\pi^2\,f_\pi^2 + O(\overline{\theta^4})$. Because of the invariance of $\mathcal{L}_\theta$ in 2.1 with respect to $\overline{\theta} \rightarrow \overline{\theta} + 2\pi$, the potential $V(\overline{\theta})$ is periodic with period 2π and consequently

Figure 2.1: Axion mixing with $\bar{q}q$ states and hence with the neutral pion π^0. The curly lines represent gluon's, the solid lines quarks. Figure borrowed from ref. [13].

$V(a)$ is periodic with $2\pi f_a$. In the PQ- scheme, $\overline{\theta}$ is a physical field, and it will therefore settle in its ground state at $\overline{\theta} = 0$.

2.2.1 Axions as Nambu-Goldstone bosons

Invariance of $\mathcal{L}_\theta$ in 2.1 against the transformation $\overline{\theta} \rightarrow \overline{\theta} + 2\pi$ and the corresponding invariance of the axion Lagrangian $\mathcal{L}_a$ against $a \rightarrow a + 2\pi f_a$ leads to the simple interpretation of the axion field as the phase of a new scalar field. This is seen most easily in the KSVZ- model which was proposed by Kim, 1979, ref. [20] and Shifman, Vainshtein and Zakharov, 1980.

The KSVZ model

The KSVZ- model gives an understanding of the structure of the couplings of axions to quarks and leptons. In this model one introduces a new complex scalar field Φ which does not take part in the weak interactions. One also introduces a new massless fermion field Ψ and considers the following Lagrangian

$$\mathcal{L} = (\frac{i}{2}\,\overline{\Psi}\,\partial_\mu\,\gamma^\mu\,\Psi + h.c.) + \partial_\mu\,\Phi^\dagger\,\partial^\mu\,\Phi - V(\mid\Phi\mid) - h\,(\overline{\Psi}_L\,\Psi_R\,\Phi + h.c.), \qquad (2.6)$$

where h.c. stands for the hermitian conjugate of the term and $\mu = 0, 1, 2, 3$. This Lagrangian contains the usual kinetic terms, a potential for the scalar field and an interaction term, but no explicit mass term for the fermion field. The parameter h is the Yukawa coupling, chosen here to be positive, and $\overline{\Psi}_L \equiv \frac{1}{2}(1 - \gamma_5)\Psi$ and $\overline{\Psi}_R \equiv \frac{1}{2}(1 + \gamma_5)\Psi$ are the left and right- handed projections of the fermion field. Left/right refers to negative/positive *helicity*. Helicity is a property of the quantum number corresponding to the spin component in the direction of movement. γ^μ are the four Dirac γ- matrices and γ_5 is a product of these [4]. The Lagrangian in 2.6 is invariant under a phase transformation of the form

[4] See ref. [16], page 102-115 for more details.

$$\Phi \to e^{i\alpha}\,\Phi, \quad \Psi_L \to e^{i\alpha/2}\,\Psi_L, \quad \Psi_R \to e^{-i\alpha/2}\,\Psi_R, \tag{2.7}$$

where α is some constant. The chiral symmetry given above is usually referred to as the Peccei- Quinn symmetry $U_{PQ}(1)$.

One chooses the potential $V(|\ \Phi\ |)$ in the Lagrangian 2.6 to be a Mexican hat potential which has an absolute minimum at $|\ \Phi\ | = (f_{PQ}/\sqrt{2})$ where f_{PQ} is some large energy scale. The ground state of the Lagrangian is characterized by a nonvanishing vacuum expectation value

$$\langle \Phi \rangle = \frac{f_{PQ}}{\sqrt{2}}\, e^{i\,\phi},$$

where ϕ is an arbitrary phase. This ground state is not invariant under a transformation of the type 2.7 and hence spontaneously breaks the PQ- symmetry.

We try to express the complex field Φ in terms of two real fields, ρ and a, representing the radial and angular excitations, respectively:

$$\Phi = \frac{(f_{PQ} + \rho)}{\sqrt{2}}\, e^{i\,a/f_{PQ}}.$$

Recall the explanation of the mass term in the Lagrangian from section 1.5.4. Since a mass term is quadratic in the fields, we see from computing $\Phi^*\Phi$ that field ρ will get a mass term associated with it, while the θ field will not. The field ρ will therefore be of no further interest for our low- energy considerations and we can neglect all terms involving ρ in the Lagrangian 2.6, which results in

$$\mathcal{L} = (\frac{i}{2}\,\overline{\Psi}\,\partial_\mu\,\gamma^\mu\,\Psi + h.c.) + \frac{1}{2}(\partial_\mu\,a)^2 - m\,(\overline{\Psi}_L\,\Psi_R\,e^{i\,a/f_{PQ}} + h.c.), \tag{2.8}$$

where we have defined $m \equiv h\,f_{PQ}/\sqrt{2}$. When performing a Peccei- Quinn transformation on this Lagrangian, the fermion fields will transform according to eq. 2.7, while the angular field transforms linearly as $a \to a + \alpha\,f_{PQ}$. The fact that the Lagrangian is invariant against these shifts is a manifestation of the $U_{PQ}(1)$ symmetry. It implies that a represents a massless particle, the so called *Nambu-Goldstone boson* of the Peccei- Quinn symmetry.

The last term in eq. 2.8 can be rewritten as

$$m\,\overline{\Psi}\,e^{i\,\gamma_5\,a/f_{PQ}}\,\Psi.$$

If one expands this term in powers of a/f_{PQ}, the zeroth order term $m\,\overline{\Psi}\,\Psi$ is the mass term for the fermion field (recall how to identify mass terms, section 1.5.4). The terms of higher order are associated with the interaction between a and Ψ, hence the following interaction Lagrangian

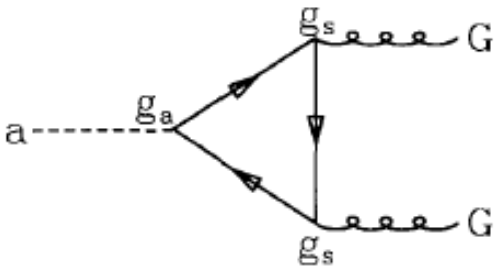

Figure 2.2: 'Triangle loop diagram for the interactions of axions with gluon's with strong coupling constant g_s and Yukawa coupling g_a of axions with the loop fermion, ref. [13].

$$\mathcal{L}_{int} = -i\,\frac{m}{f_{PQ}}\,a\,\overline{\Psi}\,\gamma_5\,\Psi + \frac{m}{2f_{PQ}^2}\,a^2\,\overline{\Psi}\,\Psi + ... \tag{2.9}$$

The fraction $m/f_{PQ} \equiv g_a$ is the relevant Yukawa coupling. Due to its proportionality with the fermion mass, in a theory with several fermion fields, the axion field will couple most strongly to the heaviest fermion.

Earlier we have seen that the term, $aG\tilde{G}$, in the axion Lagrangian implies the coupling of axions to gluon's. In order to identify the angular field a in 2.9 as the axion field, one thus needs the coupling of the fermion Ψ to gluon's. We let Ψ be some exotic heavy quark with the usual strong interactions. The lowest order interaction of a with gluon's is given by the triangular loop diagram shown in figure 2.2 . For the first order term in the interaction Lagrangian 2.9, it yields an effective a-gluon interaction of

$$\mathcal{L}_{aG} = -\frac{g_a}{m}\frac{\alpha_s}{8\pi}\,a\,G\,\tilde{G}. \tag{2.10}$$

All the external momenta were assumed to be small compared with the mass m of the fermion in the triangle loop.

In more general models, several quark fields Ψ^j may participate in the Peccei-Quinn scheme. Each field is assigned a PQ charge X_j which characterizes its $U_{PQ}(1)$ transformation, according to

$$\Psi_L{}^j \longrightarrow e^{iX_j\alpha/2}\,\Psi_L{}^j \tag{2.11}$$

This implies that the Yukawa coupling of each of these fermion fields Ψ^j to the axion field a is

$$g_{aj} = \frac{X_j\,m_j}{f_{PQ}}. \tag{2.12}$$

The total $a\,G\,\tilde{G}$- coupling is obtained from a summation of these terms over eq. 2.10. Using the following definitions

$$N \equiv \sum_j X_j, \qquad f_a \equiv f_{PQ}/N,$$

and with $\alpha_s = g_s^2/4\pi$ as defined earlier, we can rewrite the $a\,G\,\tilde{G}$ coupling in 2.10 as

$$\mathcal{L}_{aG} = -\frac{\alpha_s}{8\pi f_a}\, a\,G\,\tilde{G}$$

Comparing with eq. 2.4 it is evident that this is the required coupling which allows us to interpret the field a as the axion field.

The potential $V(a)$ is constructed to be periodic with $2\pi f_a = 2\pi f_{PQ}/N$. The interpretation of a as the phase of Φ, on the other hand, implies a periodicity with $2\pi f_{PQ}$ so that N must be a nonzero integer. This requirement restricts the possible assignment of PQ- charges to the quark fields. It also implies the existence of N different ground states for the axion field, each of which satisfies $\overline{\Theta} = 0$, and hence solves the strong CP- problem.

2.2.2 Axion models

Standard axion model

Since axions appear as the phase of a scalar field Φ, it is natural to relate Φ to the standard Higgs field. In the standard model, the Nambu- Goldstone boson that would appear from the spontaneous breakdown of SU(2) × U(1) is interpreted as the third component of the neutral gauge boson, Z^0. This means that the scalar field Φ of which axions are the phase can not be the standard Higgs field. Therefore one tries to introduce two independent Higgs fields, Φ_1 and Φ_2, with vacuum expectation values

$$\langle\Phi_1\rangle = \frac{f_1}{\sqrt{2}}, \quad \langle\Phi_2\rangle = \frac{f_2}{\sqrt{2}}.$$

The two constants f_1 and $f_2$must obey

$$\left(f_1^2 + f_2^2\right)^{1/2} = f_{weak} \equiv \left(\sqrt{2}\,G_F\right)^{-1/2} \sim 250\,\mathrm{GeV},$$

where G_F is Fermi's constant. In this so called *standard axion model*, Φ_1 gives masses to up- quarks, while Φ_2 gives masses to down- quarks and to the charged leptons. Introducing the ratio, and the number N of families of quarks, the axion decay constant is given by

$$f_a = \frac{f_{weak}}{N\ (x + 1/x)}. \tag{2.13}$$

This standard model is ruled out by experimental and astrophysical evidence, ref. [21].

Invisible axion model

Therefore, one is led to introduce an electroweak Higgs field with a vacuum expectation value

$$\langle \Phi \rangle = \frac{f_{PQ}}{\sqrt{2}}, \tag{2.14}$$

which is not related to the weak scale. Taking $f_{PQ} \gg f_{weak}$, the mass of the axion becomes very small, hence its interactions very weak. Such models are referred to as *invisible axion models*, and the KSVZ model described above is a such. Its simplicity arises from the fact that the Peccei- Quinn mechanism is totally decoupled from the ordinary particles: at low energies axions interact with matter and radiation only by virtue of their two-gluon coupling, which is generic for the PQ- scheme. In its simplest form, the KSVZ model is determined by only one free parameter, $f_a = f_{PQ}$, although one may include several quarks and then

$$f_a = \frac{f_{PQ}}{N}.$$

The DFSZ model

Another commonly used axion model is the DFSZ model which was introduced by Zhitnitskii (1980) and by Dine, Fischler, and Srednicki (1981), ref. [22]. It is a hybrid between the standard model and the KSVZ model. It uses an electroweak scalar field Φ with a vacuum expectation value $\langle \Phi \rangle = f_{PQ}/\sqrt{2}$ and two electroweak fields Φ_1 and Φ_2. There is no need for exotic quarks; only the known fermions carry Peccei- Quinn charges. In this model, $f_a = f_{PQ}/N_f$ so that in the standard picture with three families, the number of degenerate vacua is $N = N_f = 3$. The remaining free parameters of this model are f_{PQ} and $x = f_1/f_2$, the relative coupling strength to fundamental fermions. The latter is often parametrized by

$$\cos\beta = \frac{x^2}{x^2 + 1} \tag{2.15}$$

Summary

In the KSVZ- model the PQ- charge of the electron is $X_e = 0$, which means that the axions in this model (sometimes referred to as *hadronic* axions) do not couple to electrons. Therefore, from a practical perspective, the main difference between the KSVZ and DFSZ models is that in the latter axions couple to charged

leptons in addition to nucleons and photons.

There exist many other axion models and many attempts to identify the Peccei-Quinn scale with other scales. We take the approach that f_{PQ} is a free parameter that can be determined from astrophysical and cosmological experimental methods.

2.2.3 Axions interacting with ordinary matter

Axion mass and axion decay constant

In section 2.2 we found that axions pick up a small mass from its interaction with the neutral pion, as given by eq. 2.5. The exact expression was found to be (Bardeen and Tye 1978; Kandaswamy, Salomonson, and Schechter 1978; Srednicki 1985; Georgi, Kaplan and Randall; 1986, Peccei, Bardeen and Yanagida 1987)

$$m_a = \frac{f_\pi \, m_\pi}{f_a} \left[\frac{z}{(1+z+w)(1+z)} \right]^{1/2}, \tag{2.16}$$

where z and w are the quark mass ratios given as (Gasser and Leutwyler 1982)

$$z \equiv m_u/m_d = 0.568 \pm 0.042$$
$$w \equiv m_u/m_s = 0.029 \pm 0.0043.$$

Substituting the pion mass and decay constants (already stated in section 2.2), we get the following expression for the axion decay constant

$$f_a = 0.598 \times 10^7 \,\mathrm{GeV} \, \frac{\mathrm{eV}}{m_a}. \tag{2.17}$$

Or written for the axion mass

$$m_a = 0.598 \,\mathrm{eV} \, \frac{10^7 \,\mathrm{GeV}}{f_a}. \tag{2.18}$$

Axions interacting with fermions

The Lagrangian for the interaction between axions and fermions is

$$\mathcal{L}_{int} = -i \, g_{aj} \, \overline{\Psi}_j \, \gamma_5 \, \Psi_j \, a, \tag{2.19}$$

where g_{aj} is the generalized axion- fermion Yukawa coupling, which can be expressed as

$$g_{aj} = \frac{C_j m_j}{f_a}, \tag{2.20}$$

where C_j is an *effective* Peccei-Quinn charge, m_j the fermion mass and f_a is the Peccei- Quinn scale or 'axion decay constant'. Ψ_j is the wave function describing the fermion field. The *axionic fine structure constant* is

$$\alpha_{aj} = \frac{g_{aj}^2}{4\pi} \tag{2.21}$$

Numerically, the axion- fermion Yukawa coupling is

$$g_{ae} = \frac{C_e\, m_e}{f_a} = C_e\, 0.85 \times 10^{-10}\, \frac{m_a}{\mathrm{eV}}, \tag{2.22}$$

$$g_{aN} = \frac{C_N\, m_e}{f_a} = C_e\, 1.56\, \times 10^{-7}\, \frac{m_a}{\mathrm{eV}}, \tag{2.23}$$

for electrons and nucleons, respectively.

Model dependent Peccei- Quinn charges

Various axion models differ in their assignment of PQ charges, but for all of them he sum of the charges, $N = \sum_{quarks}\, X_j$, is a nonzero integer.

The assignment at high energies can not be the same as for lower energies due to the spontaneous breakdown of the electroweak symmetry, SU(2) × U(1), at $f_{EW} \cong 250\,\mathrm{GeV}$ (see section 1.5.3). The result of this symmetry breaking is the longitudinal component of the Z^0 gauge boson, which would mix with the axion. Therefore the PQ charges must be shifted such as to avoid this mixing. The shifted charges are denoted by X'_j.

Below the QCD scale $\Lambda_{QCD} \sim 200\,\mathrm{MeV}$, free quarks do not exist. Then one needs to consider the axion- nucleon coupling which arises due to the direct coupling to quarks through the mixing with π^0 (as discussed in section 2.2). This leads to the PQ charges, X'_p and X'_p, for protons and neutrons.

The above effective PQ charges are obtained by

$$C_j = \frac{X'_j}{N}, \tag{2.24}$$

in order to absorb N into the definition, just as for $f_a = f_{PQ}/N$. This definition is confirmed by the relation between the axion- fermion Yukawa couplings given in 2.20 and the one stated earlier in eq. 2.12.

In hadronic axion models, $C_e = 0$. In the DFSZ model,

$$C_e = \frac{\cos^2\beta}{N_f}, \tag{2.25}$$

normally with $N_f = 3$. Recall that the parameter β is defined in eq. 2.15 in terms of the relative coupling strength $x = f_1/f_2$.

The nucleon interactions were investigated by Kaplan (1985) and Srednicki (1985), and we only state the results. For the DFSZ model they found, with $N_f = 3$,

$$C_p = -0.10 - 0.45\,\cos^2\beta, \tag{2.26}$$

$$C_n = -0.18 - 0.39\,\cos^2\beta. \tag{2.27}$$

In the KSVZ- and other hadronic axion models

$$C_p = -0.39, \tag{2.28}$$

$$C_n = -0.04. \tag{2.29}$$

Axions interacting with photons

As explained earlier, axions mix with pions and hence couple to photons according to the following interaction Lagrangian[5]

$$\mathcal{L}_{int} = -\frac{1}{4}\, g_{a\gamma}\, F_{\mu\nu}\, \widetilde{F}^{\mu\nu}\, a = g_{a\gamma}\, \mathbf{E}\cdot\mathbf{B}\, a \tag{2.30}$$

where a is the axion field, F is the electromagnetic field strength tensor, $\tilde{F}$ its dual and $\mathbf{E}$ and $\mathbf{B}$ are the electric and magnetic fields, respectively.

As previously stated axions interact with fermions according to the interaction Lagrangian showed in eq. 2.19. When an axion interacts with two photons the amplitude of the coupling is triangular. An interaction of the form 2.19, with charged fermions, therefore automatically leads to the electromagnetic coupling in 2.30. For one fermion of charge e and mass m_j, the axion- photon Yukawa copling g_{a_γ} is (ref.[23])

$$g_{a\gamma} = \frac{\alpha}{\pi}\frac{g_{aj}}{m_j} = \frac{\alpha}{\pi f_a}\, C_{a\gamma}, \tag{2.31}$$

where $C_{a\gamma}$ is a model- dependent PQ charge, and m_j is taken to be much larger than the axion and photon energies.

In models where the quarks and leptons which carry PQ charges also carry electric charges, the total axion- photon coupling strength is (Kaplan 1985; Srednicki 1985)

[5]This Lagrangian holds unless the CP symmetry is violated.

$$g_{a\gamma} = -\frac{\alpha}{2\pi f_a}\frac{3}{4}\zeta = \frac{\zeta}{0.69\times 10^{10}\mathrm{GeV}}\,\frac{m_a}{\mathrm{eV}}, \tag{2.32}$$

where ζ is defined as

$$\zeta \equiv \frac{3}{4}\left(\frac{E}{N} - \frac{2}{3}\,\frac{4+z+w}{1+z+w}\right) = \frac{3}{4}\left(\frac{E}{N} - 1.92 \pm 0.08\right). \tag{2.33}$$

In the DFSZ model one has for a given family of quarks and leptons $E/N = 8/3$, which yields $\zeta \approx 1$.

Chapter 3

Astrophysical Axion Bounds

The existence of the axion will make an impact on stellar evolution processes. By transporting energy out of the stellar interior it may shorten the lifetime of stars. To carry away energy efficiently enough to make an impact on the evolution, the particle would have to interact weakly enough that it would stream out without being hindered too much along the way, but strongly enough that sufficiently such particles would be produced. this fact allows us to find bounds on the axion properties.

In this chapter we will study how axions couple to ordinary matter; electrons, photons and nucleons. Through the interaction with these particles, axions will be emitted and hence become a source of energy- loss in stars. We will compute the energy- loss rates by the different axion emission processes and apply the energy- loss argument relevant for the process in question. The resulting constraints on the coupling of the axion to electrons, photons and nucleons, are represented by the dimensionless Yukawa coupling, g_{ai}, which can be related to the axion properties such as the mass and decay constant.

This chapter follows the work done by Georg G. Raffelt in *Stars as Laboratories for Fundamental Physics*, ref. [1] and *Astrophysical methods to constrain axions and other novel particle phenomena*, ref. [13], closely. Our main goal is to gather the most restrictive bounds on the axion mass from its coupling to each of the constituents of ordinary matter and present how they are derived from the underlaying physics of stellar processes. The statements made with references containing a name and year of publication are references made by Raffelt in ref. [1].

3.1 Axion coupling to electrons

If axions couple directly to electrons, they can be produced thermally in stellar plasmas without nuclear processes. One of the most important quantaties which is affected by axion emission is the core mass at helium ignition. This follows from helium ignition being an extremely sensitive function of temperature. Looking at the agreement between the predicted and observationally inferred core mass, we can derive a constraint on the axion mass.

Delay of helium ignition in low mass red giants gives the most restrictive bound on the Yukawa coupling of axions to electrons g_{ae}. In the next section we will explain how this constraint is derived.

3.1.1 Delay of helium ignition in low mass red giants

The energy- loss argument

From section 1.1.2 we know that when the hydrogen burning shell deposits helium onto the core of the red giant, the core increase leads to a shrink in radius due to the degenerate conditions (see eq. 1.5). The decrease in radius results in the release of gravitational energy.

The delay is caused if an axion energy- loss rate, ϵ_a, is of the same order as the gravitational energy- loss rate, ϵ_{grav}, of the contracting core.

To get an estimate on ϵ_{grav} we treat the core of the red giant as a low mass white dwarf. The total energy of a white dwarf is found by adding its gravitational potential energy, $E_{grav} = -G\mathcal{M}/\mathcal{R}$, and its kinetic energy, obtained from the motion of the degenerate electrons as

$$E_k = N\,\frac{p_i^2}{2m_i},$$

where N is the number of electrons, p_i the momentum and m_i the mass of each electron. The result was given by Chandrasekhar (1939) as

$$E = -\frac{3}{7}\frac{G_N\mathcal{M}^2}{\mathcal{R}}. \tag{3.1}$$

To find an estimate on the radius of our low - mass white dwarf we will look at a polytropic approximation of the WD structure.

A polytropic model is a method used to simplify the equation of state to a simple relation between pressure and density[1]. Treating the degenerate Fermi

[1]For this section, the references used was ref. [2] and lecture notes written on the subject found on http://cc.oulu.fi/ jpoutane/teaching/STELL09/l07.pdf

gas of the white dwarf as one of electrons at zero temperature allows it to be described by an 'ideal fermi gas equation of state'. In the two extreme limits of i) non- relativistic electrons and ii) ultrarelativistic electrons, this equation of state reduces to its polytropic form:

$$P = K\rho_0^{\Gamma}, \tag{3.2}$$

where K and Γ are constants. The density ρ_0 is found from the sum over the product of the number density, n_i, and the mass, m_i, of each rest ion i:

$$\rho_0 = \sum_i n_i m_i.$$

Assuming the WD is a spherically symmetric mass distribution in hydrostatic equilibrium, eq. 1.1 and eq. 1.2 are satisfied. Combining these two equations reveals

$$\frac{1}{r^2}\frac{d}{dr}\left(\frac{r^2}{\rho}\frac{dP}{dr}\right) = -4\pi G\,\rho, \tag{3.3}$$

an equation satisfying both mass conservation and hydrostatic equilibrium.

Next, we substitute the equation of state 3.2 with $\Gamma = 1 + 1/n$, n being the polytropic index, into eq. 3.3, with the result

$$\frac{(n+1)}{n}\,\frac{K}{4\pi G}\,\frac{1}{r^2}\frac{d}{dr}\left(r^2\rho^{1+1/n}\frac{d\rho}{dr}\right) = -\rho. \tag{3.4}$$

Our goal is the solution of this equation $\rho(r)$ for $0 < r < R$. To find the solution it is convenient to introduce

$$\rho = \rho_c\theta^n,$$

where θ is a dimensionless variable satisfying $0 \le \theta \le 1$ and ρ_c is the density at the centre of the star. The boundary conditions are $\theta = 1$ at the centre of the star and $\theta = 0$ at the surface. We also introduce a dimensionless radius by

$$r = \alpha\,\xi, \tag{3.5}$$

where α is given by

$$\alpha = \left[\frac{(n+1)\,K\rho_c^{(1/n-1)}}{4\pi G}\right]^{1/2}. \tag{3.6}$$

We substitute these two expressions for ρ and r into eq. 3.4. The equation for mass conservation and hydrostatic equilibrium with the polytropic equation of state becomes the Lane- Emden equation for the structure of a polytrope of index n,

$$\frac{1}{\xi^2}\frac{d}{d\xi}\xi^2\frac{d\theta}{d\xi} = -\theta^n. \tag{3.7}$$

The Lane- Emden equations can be integrated numerically, starting from $\xi = 0$ with the boundary conditions on θ. The solutions for θ decrease until a point with the finite value $\xi = \xi_1$ for which $\theta(\xi_1) = 0$, thus being the surface of the star. Recall that we are after the radius, which can be found from eq. 3.5 and 3.6 with $\xi = \xi_1$.

$$R = a\xi_1 = \left[\frac{(n+1)\,K}{4\pi G}\right]^{1/2} \rho_c^{(1n-1)/2n}\,\xi_1 \tag{3.8}$$

In our case, the radius to be computed is that of a low- mass white dwarf which consits of non- relativistic electrons. The values for Γ and ξ_1 for this case were found by Chandrasekhar (1939) to be

$$\Gamma = \tfrac{5}{3}, \quad n = \tfrac{3}{2}, \quad \xi_1 = 3.65375,$$

which yields a radius of

$$R = 1.12 \times 10^4 \left(\frac{\rho_c}{10^6\, g\, cm^{-3}}\right)^{-1/6} \left(\frac{\mu_e}{2}\right)^{-5/6} \text{km}, \tag{3.9}$$

The central density for the polytropic model is given by

$$\rho_c = 1.46 \times 10^6\, g\, cm^{-3} \left(\frac{\mathcal{M}}{0.6\mathcal{M}_\odot}\right)^2 \left(\frac{\mu_e}{2}\right)^5. \tag{3.10}$$

In the last two expressions, μ_e is the mean molecular weight per electron,

$$\mu_e = \frac{m_B}{m_u}\,\mathrm{Y}_e,$$

where m_B is the mean baryon rest mass and m_u is the atomic mass unit. The distinction between the latter two can be ignored, since they are of the same order. The parameter Y_e is the mean number of electrons per baryon, defined in general as the number fraction of nuclear species per baryon:

$$\mathrm{Y}_j = \frac{Z}{A}, \tag{3.11}$$

where Z is the atomic number and A is the atomic mass[2]. Here $\mathrm{Y}_e = 0.5$ since there is no hydrogen in the WD's interior, so that the mean molecular weight becomes $\mu_e = \mathrm{Y}_e^{-1} = 2$. Substituting ρ_c into eq. 3.9, we arrive at the following simplified expression for the radius of the white dwarf star

[2]The atomic number Z is the number of protons in a nucleus, while the atomic mass A includes neutrons, i.e. it is the total number of nucleons.

$$R = R_* \frac{\mathcal{M}_\odot}{\mathcal{M}^{1/3}},$$

where $R_* = 8800\ km$.

We obtain the energy- loss rate per unit mass by taking the negative time derivative of the total energy, dividing by the mass. With the radius found (eq. 3.1.1), the result is

$$\langle \epsilon_{grav} \rangle = -\frac{\dot{E}}{\mathcal{M}} = \frac{G_N \mathcal{M}_\odot}{R_*} \left(\frac{\mathcal{M}}{\mathcal{M}_\odot} \right)^{1/3} \frac{\dot{\mathcal{M}}}{\mathcal{M}_\odot}$$

Numerical values close to the helium ignition, $\mathcal{M} \approx 0.5\ \mathcal{M}_\odot$ and $\dot{\mathcal{M}} \approx 0.8 \times 10^{-15} \mathcal{M}_\odot s^{-1}$, were found by Sweigart and Gross (1978). With these values we find a the gravitational energy- loss rate of $\langle \epsilon_{grav} \rangle \approx 100\, erg\, g^{-1} s^{-1}$. From the criterion put forward in the start of this section, this implies requiring $\langle \epsilon_x \rangle \ll 100 erg\, g^{-1} s^{-1}$ too avoid delay of helium ignition.

However, this criterion was sharpened by Sweigart and Gross (1978) and Raffelt and Weiss (1992) who studied the delay of helium ignition numerically, varying the factor F_ν describing the neutrino emission rate. $F_\nu = 1$ represents the standard case. For $F_\nu < 1$, the neutrino emission is decreased so that helium ignites earlier. The criterion put forward came from preventing the core mass from exceeding its standard value by more than 5% ($\delta \mathcal{M} < 0.025 \mathcal{M}_\odot$). For this criterion to hold, they showed that the factor $F_\nu \lesssim 3$, which leads to $\langle \epsilon_{grav} \rangle \lesssim 2 \langle \epsilon_\nu \rangle$.

According to Sweigart and Gross (1978), the neutrino luminosity of the core at helium ignition is approximately $1\, L_\odot$, so that $\langle \epsilon_\nu \rangle \approx 4\, erg\, g^{-1} s^{-1}$. They concluded with an approximate analytic criterion to constrain a nonstandard energy loss of

$$\langle \epsilon_x \rangle \lesssim 10\, erg\, g^{-1} s^{-1}. \tag{3.12}$$

Note that $\langle \epsilon_X \rangle$ must be calculated for a helium plasma with an average core density and temperature of

$$\rho_c \sim 2 \times 10^5 g\, cm^{-3}, \quad T = 10^8\, K \tag{3.13}$$

Axion emission by bremsstrahlung

Bremsstrahlung emission is important under degenerate conditions. Since it is not suppressed by degeneracy effects, as opposed to the Compton process, one can apply the helium ignition- argument derived above. That is, we can

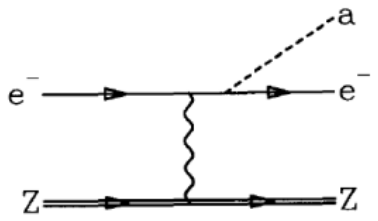

Figure 3.1: Bremsstrahlung production of axions, or for the absorption by inverse bremsstrahlung. The double line represents a nucleus of charge Ze, or another electron. Figure from ref. [13].

apply the constraint given in eq. 3.12 for axions emitted from the process of bremsstrahlung.

The bremsstrahlung process is the process of an electron interacting with the Coulomb field of a helium nucleus, see figure 3.1. We consider the process where the result is the emission of an axion through

$$e + {}^4He \longrightarrow {}^4He + e + a.$$

Under degenerate conditions the collision between the electrons can be neglected compared to the electron- nucleus interaction. For the temperature condition in eq. 3.13, but a density of $\rho \sim 10^6\, g\, cm^{-3}$, the plasma will be weakly coupled. In a weakly coupled plasma both electrons and ions will be effected by *screening*. Screening is the effect that an electric test charge will be screened by the polarization of the plasma. The plasma is polarized by the test charge because the positive constituents of the plasma are repelled while the negative ones are attracted.

With these assumptions, the axion emission rate per unit volume by bremsstrahlung was given by Raffelt (1990), as

$$Q = \frac{\pi^2 \alpha^2 \alpha_{ae}}{15} \frac{T^4}{{m_e}^2} \left(\sum_j n_j {Z_j}^2 \right) F.$$

Here α is the fine structure constant (eq. 1.54), α_{ae} is the axionic fine structure constant (eq. 2.21) and m_e is the electron mass. The sum is over all nuclear species with charges $Z_j e$ and number density n_j. F is a dimensionless function depending on angles between the momenta of the electrons and the velocity at the Fermi surface.

By dividing emission rate per unit volume Q by the density ρ, we find the

emission rate per unit mass ϵ_a. The electron number density is

$$n_e = \sum_j n_j Z_j = \frac{Y_e \rho}{m_u} = \frac{Z}{A}\frac{\rho}{m_u}.$$

The energy- loss rate per unit mass for a single species of nuclei with charge Ze and atomic weight A thus becomes

$$\begin{aligned} \epsilon_a &= \frac{\pi^2 \alpha^2 \alpha_{ae}}{15}\,\frac{Z^2}{A}\,\frac{T^4}{m_u m_e^2}\,F \\ &= \alpha_{ae}\; 1.08 \times 10^{27} erg\; g^{-1} s^{-1}\,\frac{Z^2}{A}\,T_8^4\,F \end{aligned} \tag{3.14}$$

where $T_8 = T/10^8 K$. Because F is of order unity for all the conditions, the bremsstrahlung rate mostly depends on the temperature and chemical composition, so that ϵ_a is not suppressed at high density. Assuming the plasma is degenerate, but weakly coupled, the screening scale is dominated by ions. We will use a value of $F \approx 1.8$ found by Raffelt, ref. [1][3].

Applying the Energy- loss argument

For the atomic number and weight, Z and A, in eq. 3.14, we will substitute those of the helium nucleus. With the conditions for average core density and temperature of a typical white dwarf given in 3.13, the axion emission rate becomes $\epsilon_a \approx \alpha_{ae}\, 2 \times 10^{27}\, erg\, g^{-1} s^{-1}$. Together with the requirement in eq. 3.12, we arrive at a constraint on the axionic fine- structure constant of

$$\alpha_{ae} \lesssim 0.5 \times 10^{-26}.$$

The relation between α_{ae} and the axion- electron Yukawa coupling g_{ae}, given in eq. 2.21 results in a constraint on the latter of

$$g_{ae} \lesssim 2.5 \times 10^{-13}.$$

We now want to relate this constraint on the the Yukawa coupling g_{ae} to a constraint on the Peccei- Quinn scale (f_{PQ} or $f_a = f_{PQ}/N$), and thereby on the axion mass m_a. These are related by eq. 2.22. Finally, with the relation between the axion decay constant and mass from eq. 2.17, we arrive at our result: The bounds on the axion mass and axion decay constant, obtained from the delay of helium ignition in low mass red giants that would be caused by excessive axion emission are

$$m_a C_e \lesssim 0.003\,\mathrm{eV} \tag{3.15}$$

$$f_a/C_e \gtrsim 2 \times 10^9\,\mathrm{GeV} \tag{3.16}$$

[3]The function F is given by eq. 3.34, and in this case by eq. 3.36 on page 104.

What is the PQ charge of the electron, C_e, for the different axion models? We know from section 2.2.3 that $C_e = 0$ in the KSVZ model, which implies that there are no special bounds on m_a and f_a.

In the DSFZ model, C_e is given by eq. 2.25. Taking the number of families $N_f = 3$, the bounds on the axion mass and decay constant for the DSFZ model are

$$m_a \, cos^2\beta \lesssim 0.01 \, \text{eV}$$
$$f_a/cos^2\beta \gtrsim 0.7 \times 10^9 \, \text{GeV}.$$

These limits depend on the parameter $cos^2\beta$ which can, in principle, be zero.

3.2 Axion coupling to photons

Axions couple to photons because they have a two- photon vertex. It allows for the conversion $a \longrightarrow \gamma$ in an external electric or magnetic field. This is known as the Primakoff process and in stars it allows for the emission of axions.

We saw in the previous section that the core mass at helium ignition is an important astrophysical quantity which will be affected if axions are produced and emitted in stars. Another simple argument arises from the observed duration of helium burning of low- mass stars, i.e. the lifetime of stars on the horizontal branch (recall HB stars discussed in section 1.1.2). This is the process which reveal the most restrictive bound on the interaction of axions with photons.

3.2.1 Helium burning lifetime of HB stars

Energy- loss argument found from globular cluster stars

In Raffelt, ref.[13] it is argued that the number ratio of stars on the HB versus RGB in globular clusters agreed with standard predictions to within 10%. Therefore helium- burning lifetime agrees t_{He} agrees with standard predictions to within this limit. With $L_{3\alpha}$ the standard helium- burning luminosity of the core, t_{He} will be reduced by approximate factor

$$\frac{L_{3\alpha}}{L_a + L_{3\alpha}}. \tag{3.17}$$

Demanding a reduction by less than 10% translates to a requirement $L_a \lesssim 0.1 \, L_{3\alpha}$. The standard value for the $L_{3\alpha} \sim 20 \, L_\odot$. The core mass is about $0.5 \, \mathcal{M}_\odot$, which gives a core- averaged energy generation rate of $\langle \epsilon_{3\alpha} \rangle \approx 80 \, erg \, g^{-1} s^{-1}$. Then an axion energy- loss rate is constrained by

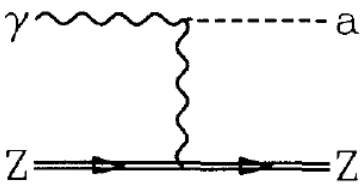

Figure 3.2: Primakoff conversion between axions and photons in an external electromagnetic field. Figure from ref. [13].

$$\langle \epsilon_a \rangle \lesssim 10\, erg\, g^{-1} s^{-1}. \tag{3.18}$$

Axion production from Primakoff conversion

In stars the Primakoff conversion of photons leads to the production of axions in the electric fields of nuclei and electrons.

The energy- loss per unit volume for the Primakoff process in a stellar plasma is

$$Q = \frac{g_{a\gamma}^2 T^7}{4\pi} F(\kappa^2). \tag{3.19}$$

Here $\kappa \equiv k_s/2T$ where k_s is the screening scale, which for a nondegenerate medium is given by the Debye- H*ü*ckel formula

$$k_s^2 = \frac{4\pi\alpha}{T} n_B \left(Y_e + \sum_j Z_j^2 Y_j \right)$$

where $n_B = \rho/m_u$ is the baryon density and Y_j is the number fraction of nuclear species per baryon in eq. 3.11. The function $F(\kappa^2)$ is ..

In the core of an HB star with density $\rho = 10^4\, g\, cm^{-3}$ and temperature $T = 10^8\, K$, Raffelt (in ref. [1]) found that $\kappa^2 \approx 2.5$ which again leads to $F \approx 1$.

As for the bremsstrahlung emission rate, we divide Q by the density to get the energy- loss rate per unit mass ϵ. For the given temperature and density, with the definition $g_{10} = g_{a\gamma} \times 10^{10}$ GeV, the axion energy- loss rate per unit mass for the Primakoff process becomes

$$\epsilon_a = g_{10}^2\, 30\, erg\, g^{-1} s^{-1} \tag{3.20}$$

Applying the Energy- loss argument

According to the constraint in eq. 3.18, with the emission rate given in 3.20, one finds the following bound on the axion- photon Yukawa coupling

$$g_{a\gamma} \lesssim 0.6 \times 10^{-10}\text{GeV}. \tag{3.21}$$

The coupling $g_{a\gamma}$ is given in equations 2.31 and 2.32. If we equate these two we can find the model dependent PQ charges to be $C_{a\gamma} = 3/8\,\zeta$. The constraint on the axion mass is obtained from axion- photon coupling given in terms of ζ in 2.32. As before we also use the relation between the axion mass and its decay constant in 2.17 to give the constraint in terms of f_a also. The results are

$$m_a\zeta \lesssim 0.4\,\text{eV} \tag{3.22}$$

$$f_a/\zeta \gtrsim 1.5 \times 10^7\,\text{GeV}. \tag{3.23}$$

In section we saw that the model dependent parameter ζ, for the DFSZ model is $\zeta \approx 1$, which gives a bound of $m_a \lesssim 0.4\,\text{eV}$

Note that the temperature $10^8\,K$ corresponds to 8.6 keV. Under these conditions a typical photon energy is $3T \approx 25.8\,\text{keV}$, thus restricting these bounds to apply to axions with masses $m_a \lesssim 30\,\text{keV}$.

3.3 Axion coupling to nucleons

The most restrictive limit on the axion- nucleon coupling arises from the observed duration of the neutrino signal of the supernova SN 1987A.

3.3.1 Duration of the neutrino signal of the supernova SN 1987 A

Recall from section 1.1.2 that when a massive star explodes in a type II supernova explosion, the main output of energy is a burst of neutrinos. The duration of the neutrino burst can be affected by emission of axions.

Examples of the processes where axions are emitted in nuclear media are emission by bremsstrahlung $N\,N \longrightarrow N\,N\,a$ and the Compton process $\gamma\,p \longrightarrow p\,a$.

The coupling of axions to nucleons is found from the axion- fermion interaction in eq. 2.19 as $\mathcal{L}_{int} = -i\,g_{aN}\,\overline{\psi}_N\,\gamma_5\,\psi_N$, where $\overline{\psi}_N$ is the nucleon Dirac field and m_N the nucleon mass.

This interaction rate can be applied to find the energy- loss rate per unit mass for the bremsstrahlung emission of axions,

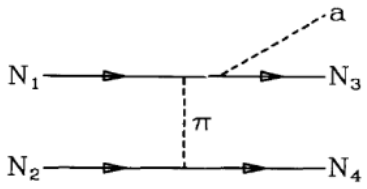

Figure 3.3: Nucleon bremsstrahlung production of axions. Figure from ref. [13].

$$\epsilon_a = \alpha_{aN}\, 1.69 \times 10^{35}\, erg\, g^{-1} s^{-1} \rho_{15}\, T_{MeV}^{3.5},$$

assuming nondegenerate conditions. Here $\rho_{15} = \rho/10^{15} g\, cm^{-3}$ and $T_{MeV} = T/MeV$. For typical core conditions of $T \approx 30\,\mathrm{MeV}$ and $\rho \approx 3 \times 10^{14}\, g\, cm^{-3}$, the energy- loss rate becomes

$$\epsilon_a = g_{aN}^2\, 10^{38}\, erg\, g^{-1} s^{-1}. \tag{3.24}$$

where α_{aN} is the axion- nucleon fine structure constant given in general for fermions in eq. 2.21.

In order to estimate the impact on the neutrino signal from cooling by axion emission, it is useful to calculate the neutrino signal from a numerical study of an evolving neutron star. This method leads to the following exclusion of the yukawa coupling constant

$$1 \times 10^{-10} \lesssim g_{aN} \lesssim 3 \times 10^{-7} \tag{3.25}$$

Since no reliable calculations of the axion emission rate from a nuclear medium is available at this time, it could be just as useful to perform a simple analytic estimate. Approximately one second after the core bounce, the neutrino luminosity is about $L_\nu = 3 \times 10^{52}\, erg\, g^{-1} s^{-1}$. With a mass of the object of around $1.5 \mathcal{M}_\odot$, its average energy- loss rate is approximately $L_\nu/\mathcal{M} \approx 1 \times 10^{19}\, erg\, g^{-1} s^{-1}$. An axionic energy- loss rate must be of this size to shorten the duration of the neutrino signal, hence leading to the following bound on the axion emission

$$\epsilon_a \lesssim 10^{19}\, erg\, g^{-1} s^{-1}. \tag{3.26}$$

With the energy- loss rate given in eq. 3.24 and the analytic bound in 3.26, one needs to require $g_{aN} \lesssim 3 \times 10^{-10}$. With the constraint in eq. 3.25 one may altogether adopt

$$3 \times 10^{-10} \lesssim g_{aN} \lesssim 3 \times 10^{-7}. \tag{3.27}$$

as the range of the axion- nucleon Yukawa coupling excluded by the duration of the neutrino signal from SN 1987 A.

As for the previous constraints, we will also find the excluded range in terms of the axion- mass and decay constant. Recalling that the axion- nucleon Yukawa coupling g_{aN} given in eq. 2.23, we get

$$0.002\,\text{eV} \lesssim C_N\, m_a \lesssim 2\,\text{eV},$$
$$3 \times 10^6\,\text{GeV} \lesssim f_a/C_N \lesssim 3 \times 10^9\,\text{GeV}.$$

C_N with $N = n, p$ is the model- dependent coupling constant which is stated for different axion models in section 2.2.3. These bounds were derived assuming equal couplings to protons and neutrons. However, we see from equations 2.28 and 2.29 that KSVZ axions essentially do not couple to neutrons while $C_p = -0.39$. For DFSZ axions the couplings vary with $\cos^2\beta$. For $\cos^2\beta \approx 0.5$ we get approximately the same values as for the KSVZ axions. The values of the KSVZ axions in eq. 2.26 are thus taken to be generic. Assuming a proton fraction of about 0.3, Raffelt estimates an effective nucleon coupling of $C_N \approx 0.3^{1/2}\, 0.39 \approx 0.2$. For $C_N = 0.2$ the bounds become

$$0.01\,\text{eV} \lesssim m_a \lesssim 10\,\text{eV} \tag{3.28}$$
$$0.6 \times 10^6\,\text{GeV} \lesssim f_a \lesssim 0.6 \times 10^9\,\text{GeV}. \tag{3.29}$$

In the next chapter we will apply cosmological aspects to derive bounds on the axion mass. Figure 4.1.3 at the end of the chapter shows a summary of both astrophysical and cosmological bounds.

Chapter 4

Cosmological axion bounds

In this chapter we will deduce the expression for the present density parameter Ω_X for a general dark matter candidate according to the generic WIMP scenario. By inferring the properties of the axion, we obtain the axion density parameter Ω_a. This will be compared to observational results in order to obtain a bound on the axion mass.

The chapter also includes a brief qualitative study the evolution of the axion field, for the case of inflation occurring

4.1 Freeze- out of dark matter

For much of its early history, most constituents of the Universe were in thermal equilibrium. If a massive particle species remained in thermal equilibrium until today its abundance (see eq. 1.32), $n \propto exp(-m/T)$, would be absolutely negligible due to the decrease in temperature. However, there have been a number of notable departures from equilibrium, such as neutrino decoupling, decoupling of the CMB and primordial nucleosynthesis. If not for such departures from equilibrium, the present universe would be completely specified by the present temperature.

The rough criterion for a particle species to be either coupled or decoupled involves a comparison between the interaction rate of the particle, Γ, with the expansion rate of the Universe, H. For $\Gamma \gg H$, the particle is coupled while for $\Gamma \ll H$, the particle will decouple, or *freeze- out*. Note that the Γ involved is the interaction rate for the reaction(s) that keep the particle species in question in equilibrium. If freeze- out occurs at a temperature such that m/T (in natural units) is not much greater than 1, the species could have a significant relic abundance today, [11].

The dark matter candidates produced in the early universe are called cosmic

relics and can be categorized into thermal and non-thermal relics. Thermal relics are in thermal equilibrium with the rest of the universe until they decouple; a good example, although not a dark matter candidate, is the neutrino. One can subdivide this class into hot and cold relics according to whether they are relativistic or not when they decouple. Non-thermal relics are not produced in thermal equilibrium with the rest of the universe, but rather created by some nonthermal process.

Relic axions are created through both thermal and non-thermal processes, (Kolb and Turner, 1994, [11]). The thermal production channel is the standard WIMP scenario, which will be explained in detail in chapter 4.1.1. Non-thermal production of axions happens through the so called *misalignment production* and will only be described qualitatively in section 4.1.2. Axions are also produced non-thermally through the decay of *cosmic axion strings*, here discussed briefly in section

The two most prominent references used for this chapter was *Modern Cosmology* by Dodleson, [4], *The Early Universe* by Kolb and Turner, [11] and *Stars as Laboratories for Fundamental Physics* by Raffelt, ref. [1].

4.1.1 Thermal production

The Boltzmann equation can be used to calculate how the relic abundance of a heavy dark matter candidate X changes with time in the expanding universe.

The standard WIMP scenario

In the WIMP (weakly- interacting massive particle) scenario we study two heavy dark matter particles X that can annihilate producing two light leptons l by the process $X + X \longrightarrow l + l$. The leptons will be tightly bound to the cosmic plasma and can be taken to be in both chemical, i.e. the chemical potentials on each side of the reaction balance, and kinetic equilibrium (scattering processes are so rapid that the particle distributions take on their equilibrium forms). Hence, their number density is given by the thermal equilibrium distribution $n_l = n_l^{(0)}$. The Boltzmann equation, 1.41, for this process becomes

$$a^{-3}\,\frac{d(n_X\,a^3)}{dt} = \langle\sigma_A v\rangle\,\left\{(n_X^{(0)})^2 - n_X^2\right\}. \tag{4.1}$$

Recall, from the section on the Boltzmann equation, that $\langle\sigma_A v\rangle$ is the product of the annihilation cross section and the relative velocity. For simplicity, it will henceforth be referred to as the *thermally averaged cross section*.

During the first few tens of thousands of years the energy density of the universe is dominated by its radiation component. The energy density of a gas of

ultrarelativistic particles is proportional to T^4 and the variation of the energy density with the scale factor is for radiation is $\rho c^2 \propto a^{-4}$, hence the inverse proportionality between the temperature and the scale factor $T \propto a^{-1}$. To go further we can use this fact by dividing and multiplying the factor $(n_X a^3)$ inside the brackets on the left- hand side of eq. (4.1) by T^3 and thus remove $(aT)^3$ outside the derivation. Defining

$$Y \equiv \frac{n_X}{T^3},$$

the differential equation 4.1 becomes

$$\frac{dY}{dt} = T^3 \langle \sigma_A v \rangle \left\{ Y_{EQ}^2 - Y^2 \right\}, \tag{4.2}$$

with $Y_{EQ} \equiv n_X^{(0)}/T^3$. To go further it is convenient to introduce a new variable, $x \equiv m_X c^2/k_B$, where m_X is the mass of the heavy particle. Very high temperature corresponds to $x \ll 1$, in which case reactions proceed rapidly so $Y \simeq Y_{EQ}$. In the non- relativistic limit; when the temperature drops below the mass of the X particle, the number density becomes suppressed by the exponential factor e^{-x}. It thus becomes more and more difficult for an X particle to find a partner to annihilate with and hence they eventually drop out of equilibrium. To rewrite the differential equation (4.2) with regards to our new time variable, we remember that $T \propto a^{-1}$, so that we can substitute $T = (C\,a)^{-1}$ and write

$$\begin{aligned} \frac{d}{dt} &= \frac{dx}{dt}\frac{d}{dx} = \frac{d}{dt}\,(m\,C a)\,\frac{d}{dx} = \frac{da}{dt}\frac{d}{da}\,(m\,C a)\frac{d}{dx} \\ &= \frac{\dot{a}}{a}\,m\,C\,a\frac{d}{dx} \\ &= Hx\frac{d}{dx}. \end{aligned} \tag{4.3}$$

Since we can expect freeze- out of dark matter to take place in the radiation dominated era (see section 3.3.5), the energy density will be given by eq. 1.36. We can therefore rewrite the Hubble parameter H as

$$H = \frac{H(k_B = mc^2)}{x^2} \equiv \frac{H(m)}{x^2} \tag{4.4}$$

The condition for freeze- out is, as explained in the beginning of this chapter, $\Gamma \simeq H$, where $\Gamma \propto \langle \sigma_A v \rangle$. We incorporate this into our calculations with the ratio of the annihilation cross section and the expansion rate, parametrized by

$$\lambda \equiv \left(\frac{m_X c^2}{k_B} \right)^3 \frac{\langle \sigma_A v \rangle}{H(m)}. \tag{4.5}$$

The evolution equation then becomes

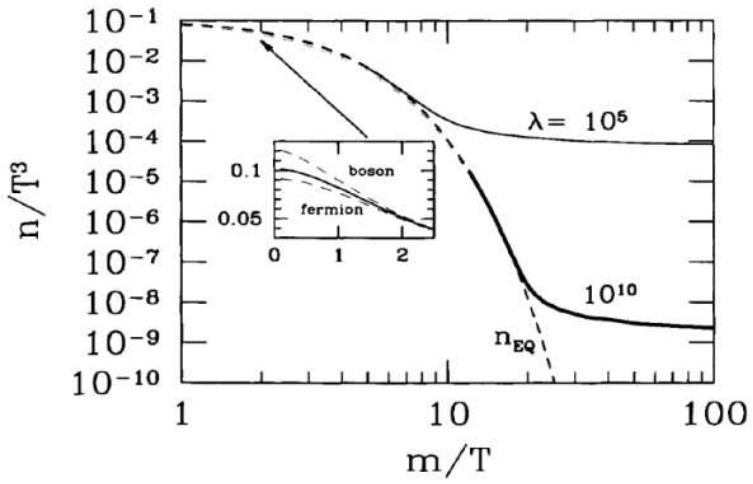

Figure 4.1: Abundance of heavy stable particle as the temperature drops. Figure taken from [4]

.

$$\frac{dY}{dx} = -\frac{\lambda}{x^2}\left\{Y^2 - Y_{EQ}^2\right\}. \tag{4.6}$$

There is in general no analytic solution for equation 4.6. Figure 4.1 shows the numerical solution to eq. (4.6) for several different values of λ. To solve this equation we can make use of our understanding of the freeze- out process to get an expression for the final freeze-out abundance $Y_\infty \equiv Y(x = \infty)$. The thermally averaged cross section, $\langle\sigma_A v\rangle$, may be temperature dependent, but if we assume it is a constant we'll be able to get some features of the solution of this equation. When $x \sim 1$, the left- hand side of the equation is of order $\sim Y$, while the right hand side is of order $Y^2\lambda$. Since λ is typically $\gg 1$, the equality is maintained only with $Y = Y_{EQ}$. Later, as the temperature drops and x increases, Y_{EQ} is no longer a good approximation to Y. After the freeze-out, $Y \gg Y_{EQ}$, as particles are not able to annihilate fast enough to maintain equilibrium. The equation is then reduced to

$$\frac{dY}{dx} \approx -\frac{\lambda Y^2}{x^2}. \tag{4.7}$$

Integrating this from the epoch of freeze-out at x_f up to very late times, i.e. as $x \longrightarrow \infty$:

$$\int_{Y_f}^{Y_\infty} \frac{dY}{Y^2} = -\lambda \int_{x_f}^{\infty} \frac{dx}{x^2}. \tag{4.8}$$

The result,

$$\frac{1}{Y_\infty} - \frac{1}{Y_f} = \frac{\lambda}{x_f}, \tag{4.9}$$

can, by noting that Y_f is significantly larger than Y_∞, be simplified to

$$Y_\infty = \frac{x_f}{\lambda}. \tag{4.10}$$

After freeze-out, the energy density of the heavy dark matter particle decays with the expansion of the universe as a^{-3}, see equation (1.23):

$$\rho_X(a_0) = \rho_X(a_1)\left(\frac{a_1}{a_0}\right)^3,$$

where a_1 is the scale factor when Y reaches Y_∞ and a_0 is its present value. The energy density in this non-relativistic regime at $a = a_1$ is given by equation 2.14. The number density at that time is $n_X(a_1) = Y_\infty T_1^3$, hence we get

$$\rho_X c^2 = n_X(a_1)\, m_X c^2 \left(\frac{a_1}{a_0}\right)^3 = m_X c^2\, Y_\infty T_1^3 \left(\frac{a_1}{a_0}\right)^3.$$

We now divide and multiply by the current CMB temperature T_0, hence

$$\rho_X c^2 = m_X c^2\, Y_\infty T_0^3 \left(\frac{a_1 T_1}{a_0 T_0}\right)^3. \tag{4.11}$$

Opposed to what we first would expect seeing we assumed $T \propto a^{-1}$, the ratio $a_1 T_1 / a_0 T_0$ does not remain constant throughout the evolution of the universe. The photons are heated by the annihilation's of many particles with masses between 1 and 100 MeV, thus raising the temperature of the Universe. The ratio $(a_1 T_1)/(a_0 T_0)$ can be computed from conservation of entropy density. From equation 1.40 we see that the wanted ratio can be computed from

$$\left(\frac{a_1 T_1}{a_0 T_0}\right)^3 = \frac{g_{*s}(a_0)}{g_{*s}(a_1)}$$

Without making too much of an error, we will use the values for g_*. The value for the present effective relativistic degrees of freedom was found in section 1.3.6 to be $g_*(a_0) = 3.36$. If we assume $k_B T_1 \sim 10\,\mathrm{GeV}$, the contribution from quarks and antiquarks is $2 \times 5 \times 3 \times 2 = 60$. Leptons contribute $2 \times 6 \times 2 = 24$ in addition to photons contributing $g_\gamma = 2$ and gluon's 8×2 (the latter to are bosons), resulting in

$$g_*(a_1) = 2 + 16 + \frac{7}{8}(60 + 24) = 91.5$$

From entropy conservation one thus find $(3.36/91.5)^3 \simeq 1/30$, and eq. 4.11 becomes

$$\rho_X\, c^2 \approx \frac{m_X c^2\, Y_\infty T_0^3}{30}$$

To find the fraction of the critical density contributed today by the heavy dark matter candidate X, we insert our expression for Y_∞ and divide by ρ_{crit} to get

$$\Omega_X = \frac{x_f}{\lambda}\frac{m_X\, T_0^3}{30\,\rho_{crit}}.$$

Substituting the expression for λ yields

$$\Omega_X = \frac{H(m)}{\langle\sigma_A v\rangle}\left(\frac{k_B}{m_X c^2}\right)^3 \frac{x_f\, m_X T_0^3}{30\,\rho_{crit}}. \tag{4.12}$$

By the definition in 4.4, $H(m)$ is the Hubble rate at the time when the temperature was equal to the mass, i.e. when $mc^2 = k_B$. We can compute it from the first Friedmann equation (eq. 1.12), as $H = \sqrt{(8\pi G/3)\,\rho}$. Substituting for the energy density given in (eq. 1.36) results in

$$H(m) = \left[\frac{8\pi G}{3}\,\rho\,(mc^2 = k_B)\right]^{1/2} = \left[\frac{4\pi^3 G\, g_*}{45}\left(\frac{c}{\hbar}\right)^3\right]^{1/2} m_x^2,$$

leading to the present density parameter for the dark matter candidate X,

$$\Omega_X = \left[\frac{4\pi^3 G\, g_*}{45}\left(\frac{c}{\hbar}\right)^3\right]^{1/2}\left(\frac{k_B}{c^2}\right)^3 \frac{x_f T_0^3}{30\,\langle\sigma v\rangle\,\rho_{crit}}. \tag{4.13}$$

The present value of the critical energy density was given in 1.16 as $\rho_{crit} = 1.879\times 10^{-29}\, h^2 g\, cm^{-3}$ and the current temperature of the CMB radiation is $T_0 = 2.725K$. Inserting these values, we obtain the axion density parameter as a function of the axion mass, the freeze-out temperature and the thermally averaged annihilation cross section as

$$\Omega_X h^2 = 5.35\times 10^{-37}\, g_*^{1/2}\left[\frac{\mathrm{MeV}}{T_f}\right]\left[\frac{cm^3 s^{-1}}{\langle\sigma_A v\rangle}\right]\left[\frac{m_X}{\mathrm{eV}}\right]. \tag{4.14}$$

We are left with four variables; the effective number of relativistic degrees of freedom, g_*, the freeze out temperature, T_f, the thermally averaged cross section, $\langle\sigma_A v\rangle$ (recall that this actually is a product of a cross section and a velocity, thereby the units), and the mass of the dark matter candidate, m_X. In order to get further we consider a specific particle species, namely our axion. The cross section is related to both the freeze- out temperature and the axion mass. It is thus necessary to look at a specific process for the axion production in order to find this relation.

For temperatures below 200 MeV

The most important process for thermal axion production is pion- axion conversion: $N + \pi \leftrightarrow N + a$. Nucleons are not present in the Universe until after the quark-hadron transition (neutrons are formed at the quark- hadron transition, i.e. when composite particles, hadrons, start forming from the quark-gluon soup), which occurs at a temperature of $T \simeq 200\,\mathrm{MeV}$. Therefore this process is only a dominant source of axion production at temperatures below this value. The cross section for the pion- axion conversion is [11]

$$\langle \sigma_A v \rangle \sim g_{aN}^2 \left(\frac{T}{m_N} \right)^2 m_\pi^{-2}, \tag{4.15}$$

where g_{aN} is the Yukawa coupling constant for the axion- nucleon interaction given in eq. 2.23. Substituting the expression for the axion decay constant, f_a from eq. (2.17), one finds

$$\langle \sigma_A v \rangle \sim \frac{T^2}{m_\pi^2} \left[\frac{(m_a/\mathrm{eV})}{0.598 \times 10^7\,\mathrm{GeV}} \right]^2 .$$

With $m_\pi = 135\,\mathrm{MeV}$, the mass of the neutral pion, this becomes

$$\langle \sigma_A v \rangle \sim \left[\frac{T}{\mathrm{MeV}} \right]^2 \left[\frac{m_a}{\mathrm{eV}} \right]^2 1.53 \times 10^{-36}\,\mathrm{eV}^{-2}.$$

Dimensional analysis suggests the correct expression for the cross section is

$$\langle \sigma_A v \rangle = \hbar^2 c^3 \left[\frac{T}{\mathrm{MeV}} \right]^2 \left[\frac{m_a}{\mathrm{eV}} \right]^2 1.53 \times 10^{-36}\,\mathrm{eV}^{-2}.$$

Inserting numbers for the constants we arrive at the final expression for the thermally averaged cross section as a function of the freeze- out temperature and the axion mass,

$$\langle \sigma_A v \rangle = 1.79 \times 10^{-35}\, cm^3 s^{-1} \left[\frac{T}{\mathrm{MeV}} \right]^2 \left[\frac{m_a}{\mathrm{eV}} \right]^2 . \tag{4.16}$$

The cross section is proportional to the square of the temperature. This is to be expected since higher temperature leads to more interactions (remember that $\Gamma \propto \langle \sigma_A v \rangle$). For this thermally averaged cross section, the axion density parameters is

$$\Omega_a h^2 = 2.98 \times 10^{-2}\, g_*^{1/2} \left[\frac{\mathrm{MeV}}{T_f} \right]^3 \left[\frac{\mathrm{eV}}{m_a} \right]. \tag{4.17}$$

We now want to compare this theoretical result with observations from the seven- year WMAP data stated in section 3.3.4. (check this) Assuming the axion accounts for 100% of the cold dark matter density, we can equate its density parameter with the one of the CDM to get $\Omega_a = \Omega_{c0} = 0.222 \pm 0.026$. The product

of the density parameter with the dimensionless hubble parameter squared is also given from the same data as $\Omega_a h^2 = \Omega_{c0} h^2 = 0.1109 \pm 0.0056$. With the values stated, the expression for the axion mass is

$$m_a = \frac{2.98 \times 10^{-2}}{0.1109 \pm 0.0056} eV \, g_*^{1/2} \left[\frac{\text{MeV}}{T_f}\right]^3 . \tag{4.18}$$

Effective number of relativistic degrees of freedom

To find out which values to use for the effective relativistic degrees of freedom g_*, we will use the results of Wantz and Shellard, [12]. They give the following expression for the effective number of relativistic degrees of freedom.

$$g_{*,R} = \sum_i \left(\frac{T_i}{T}\right)^4 \frac{15\, g_i}{\pi^4} \int_0^\infty \frac{\sqrt{x^2 + y_i^2}}{exp\sqrt{x^2 + y_i^2} + (-1)^{Q_i}} dx,$$

where $y_i = m_i/T$ and Q_i (fermion) = 1 and Q_i (boson) = 0. The numerical integration of this equation is too slow, but Wantz and Shellard approximated the exact result by fits given by the following expression

$$g_{*,i} = \exp\left[a_0^i + \textstyle\sum_{j=1}^5 a_{j,1}^i \left\{1.0 + \tanh \frac{t - a_{j,2}^i}{a_{j,3}^i}\right\}\right], \quad t = \log \frac{T}{1\,GeV} \tag{4.19}$$

The parameters a_j^i for $i = R$ are given in table 4.1.1. The fits are plotted in figure 4.2 and are generically accurate to about 1%, except at the QCD phase transition and the electron- positron annihilation[1] where the error rises to about 4%. Note that the subscript $_R$ is used to distinguish the effective number of degrees of freedom for the radiation density from the one for entropy density, $g_{*,S}$ (stated in eq. 1.39). Wantz and Shellard also analysed the $g_{*,S}$ function, but we will not go into this here.

Since we are considering the two cases of temperatures above and below 200 MeV, we will concentrate on determining values of g_* for these two cases. From eq. 4.19, we compute of $g_*(T)$ for four different temperatures, and get the following result:

T(GeV)	$\mathbf{g_*}$**(T)**
10^{-2}	20.6
50^{-2}	39.1
10^{-1}	66.5
1	76.1

[1]Electron- positron annihilation is the process when these two particles interact and the result is two photons: $e^- + e^+ \rightarrow \gamma + \gamma$

Table 4.1: Parameters for the approximation in eq. (4.19)

j	1	2	3	4	5
a_0^R	1.21	1.21	1.21	1.21	1.21
$a_{j,1}^R$	0.572	0.330	0.579	0.138	0.108
$a_{j,2}^R$	-8.77	-2.95	-1.80	-0.162	3.76
$a_{j,3}^R$	0.682	1.01	0.165	0.934	0.869

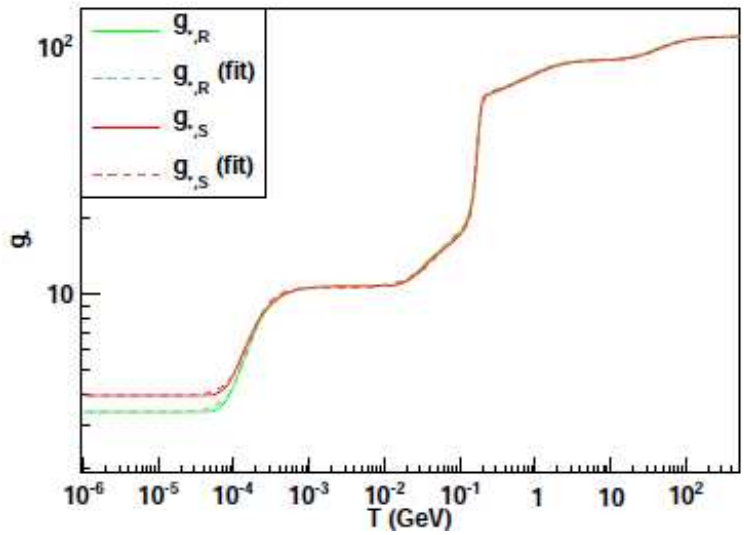

Figure 4.2: Effective number of relativistic degrees of freedom for radiation energy density, $g_{*,R}$, and entropy density, $g_{*,S}$,as a function of temperature T(GeV). Figure taken from [12]

.

Studying the plot in figure 4.2, we see that g_* has a sharp increase in the temperature range of $T \approx 100\,\text{MeV}$ to $T \approx 400\,\text{MeV}$, as already predicted. This corresponds to the QCD phase transition. It is natural to use values from the more stable regions before and after the phase transitions in our two cases, which is why we choose to utilize $g_*(T = 10\,\text{MeV}) = 20.6$ in the $T \lesssim 200\,\text{MeV}$ case and $g_*(T = 1\,\text{GeV}) = 76.1$ for $T \gtrsim 200\,\text{MeV}$.

With the determination of the parameter g_*, we can now finalize the computations by substituting $g_* = 20.6$ into 4.18 and get the following upper and lower bounds on the axion mass, respectively

$$m_a^- = 1.29\,eV \left[\frac{\text{MeV}}{T_f}\right]^3 \tag{4.20}$$

$$m_a^+ = 1.16\,eV \left[\frac{\text{MeV}}{T_f}\right]^3. \tag{4.21}$$

The exact temperature at which axions freeze-out is not known. This leads us to concider a range of temperatures; here $T_f \cong 30 - 50\,MeV$ as computed by S. Chang and K. Choi, [24].

In figure 4.3, the two expressions (4.21) and (4.20) for the axion mass are plotted as a function of freeze- out temperature. The curve shows that more massive axions will freeze out at lower freeze- out temperatures, i.e. at a later time. The reason is that all of the axion couplings, $g_{aj} \propto 1/f_A \propto m_a$, (see eq. 2.20). Hence the more massive axions are coupled more strongly and thus freeze out later.

For a freeze- out temperature of $T_f = 40\,\text{MeV}$, the bound on the axion mass becomes $1.8 \times 10^{-2}\,\text{meV} < m_a < 2.0 \times 10^{-2}\,\text{meV}$.

For temperatures above 200 MeV

At higher temperatures, $T \gtrsim 200\,\text{MeV}$, (before the QCD phase transition) there are no nucleons or pions only a quark- gluon soup and the dominant axion production process is photo- production (or gluon- production): $a + q \leftrightarrow q + \gamma$ (or $a + q \leftrightarrow q + g$). Provided the quarks are relativistic, the cross section for this process is [11]

$$\langle \sigma_A v \rangle \sim \alpha\, g_{aQ}^2\, T^{-2}, \tag{4.22}$$

where α is the fine structure constant (1.54) and g_{aQ} is the Yukawa coupling constant for the axion- quark interaction, given from eq.2.20. We substitute the expression for the axion decay constant, f_a, in terms of the axion mass given in eq. 2.17 and obtain

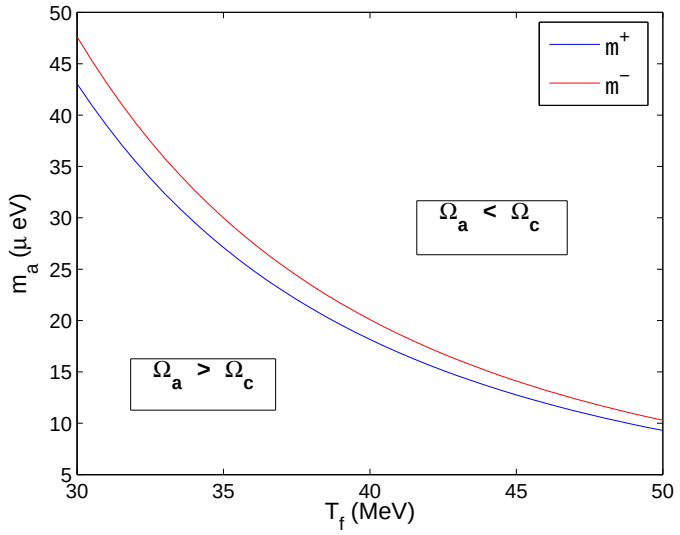

Figure 4.3: Upper and lower bounds on the axion mass as a function of freeze-out temperatures, $30 > T_f > 50$, for the process of pion- axion conversion with $g_* = 20.6$. Computed from comparison with 7-year WMAP data.

$$\langle \sigma_A v \rangle \sim \alpha \frac{m_Q^2}{T^2} \left[\frac{(m_a/\mathrm{eV})}{0.598 \times 10^7 \,\mathrm{GeV}} \right]^2 .$$

As previously, dimensional analysis is performed to get the right dimensions, i.e. adding the suitable constants, and the result is

$$\langle \sigma_A v \rangle = \alpha \hbar^2 c^3 \frac{m_Q^2}{T^2} \left[\frac{(m_a/\mathrm{eV})}{0.598 \times 10^7 \,\mathrm{GeV}} \right]^2 .$$

The masses of the quarks of different flavor range from $\sim 2\,\mathrm{MeV}$ to $\sim 200\,\mathrm{GeV}$. We will compute the cross section for two different quark masses, choosing from the bottom and top of the range. First we compute the cross section for a quark mass of $m_Q = 5\,\mathrm{MeV}$ and get

$$\langle \sigma_A v \rangle = 5.95 \times 10^{-32} \, cm^3 \, s^{-1} \left[\frac{\mathrm{MeV}}{T} \right]^2 \left[\frac{m_a}{\mathrm{eV}} \right]^2 . \tag{4.23}$$

Notice that the cross section in this case is proportional to the inverse of the square of the temperature. This means that the interaction rate decreases as the temperature increases, i.e. that quarks interact weakly at high energies, a property of QCD called *asymptotic freedom*.

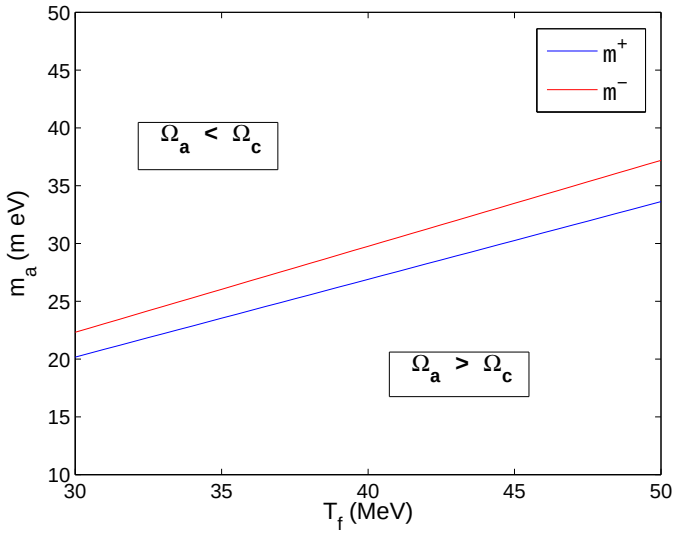

Figure 4.4: Upper and lower bounds on the axion mass as a function of freeze- out temperatures, $30 > T_f > 50$, for the axions produced via photo/gluon- production with $g_* = 76.1$. Computed from comparison with 7-year WMAP data.

Substituting this thermally averaged cross section, for $T = T_f$, into eq. 4.14, we obtain the axion density parameter,

$$\Omega_a h^2 = 8.98 \times 10^{-6}\, g_*^{1/2} \left[\frac{T_f}{\text{MeV}}\right] \left[\frac{\text{eV}}{m_a}\right]. \tag{4.24}$$

With the values from the WMAP-7 and $g_* = 76.1$, the axion mass becomes

$$m_a = \frac{8.98 \times 10^{-6}}{0.1109 \pm 0.0056}\,\text{eV}\, g_*^{1/2} \left[\frac{T_f}{\text{MeV}}\right],$$

hence revealing the following two expressions for the upper and lower axion bound, respectively

$$m_a^- = 7.44 \times 10^{-4}\, eV \left[\frac{T_f}{\text{MeV}}\right] \tag{4.25}$$

$$m_a^+ = 6.72 \times 10^{-4}\, eV \left[\frac{T_f}{\text{MeV}}\right]. \tag{4.26}$$

Repeating the same calculations, but with a quark mass of $m_Q = 180\,\text{GeV}$, reveals the following expression for the axion mass:

$$m_a = 9.80 \times 10^{-13}\,\text{eV} \left[\frac{T_f}{\text{MeV}}\right].$$

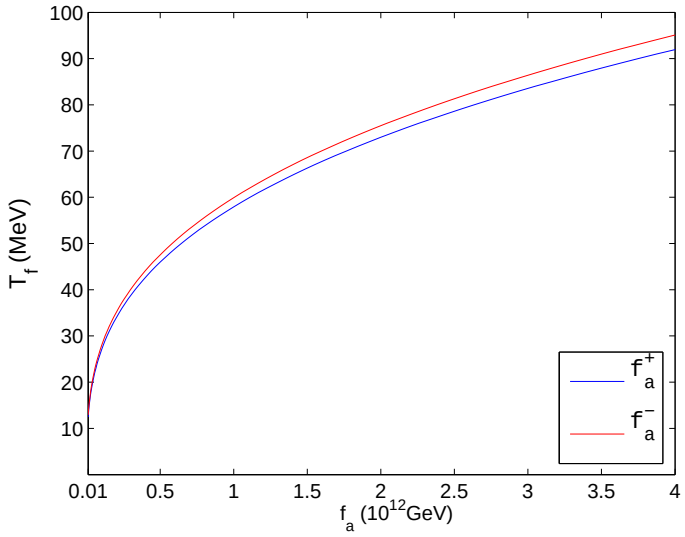

Figure 4.5: Freeze out temperature as a function of f_a for pion- axion conversion with $g_* = 20.6$

From the requirement that the quark must be relativistic for the validity of eq. 4.22, we choose to go further only with our computations based on the smaller quark mass. This is to be certain that the quark is relativistic at the temperatures in question. Figure 4.4 show the upper and lower bounds for the axion mass, (4.26) and (4.25), produced by interactions with quarks of mass $m_Q = 5\,\text{MeV}$. As opposed to the scenario of pion- axion conversion, we see from the plot that the more massive axions freeze- out at higher temperatures, i.e. at earlier times. This is due to the quarks, already mentioned, property of asymptotic freedom.

For a freeze- out temperature of $T_f = 40\,\text{MeV}$, the bound on the axion mass becomes $26.9\,\text{meV} < m_a < 29.8\,\text{meV}$.

Figures 4.5 and 4.6 show plots of the freeze-out temperature versus the axion decay constant, f_a, for the two scenarios. They show the same result as the two previous plots. For axion- pion conversion, higher axion decay constant f_a means less coupled axions which thus freeze- out earlier (at higher freeze- out temperatures). For photo/gluon production, higher f_a means the axions are more strongly coupled and thus freeze- out at a later time.

In figure 4.7 we have plotted the thermally averaged cross section $\langle \sigma_A v \rangle$ for pion- axion conversion as a function of axion mass for three different freeze- out temperatures, $T_f = 30\,\text{MeV}$, $T_f = 40\,\text{MeV}$ and $T_f = 50\,\text{MeV}$. Figure 4.8 presents

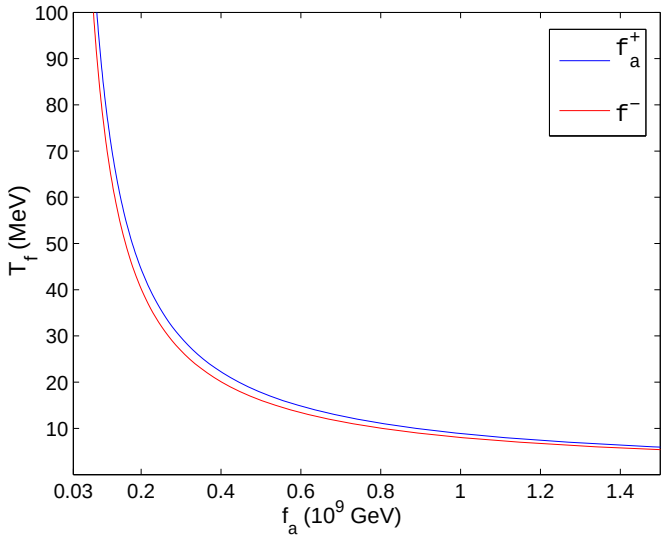

Figure 4.6: Freeze out temperature as a function f_a, for the axions produced via photo/gluon- production with $g_* = 76.1$

the same plot for photon/gluon production. As expected, the cross section increases the greater the axion mass is. Comparing two axions of the same mass, the one with the largest cross section will freeze out at a lower temperature, i.e. at a later time. This is what we expect since axions of higher cross section will interact more with other particles and thus freeze- out later.

Figure 4.9 is a plot of the axionic density parameter, $\Omega_a h^2$, as a function of axion mass for three distinct freeze-out temperatures, for the process of pion-axion conversion. The same plot for photo/gluon- production is shown in figure 4.10. The values for the density parameter of cold dark matter, $\Omega_c h^2$, from the WMAP data are the two black horizontal lines.

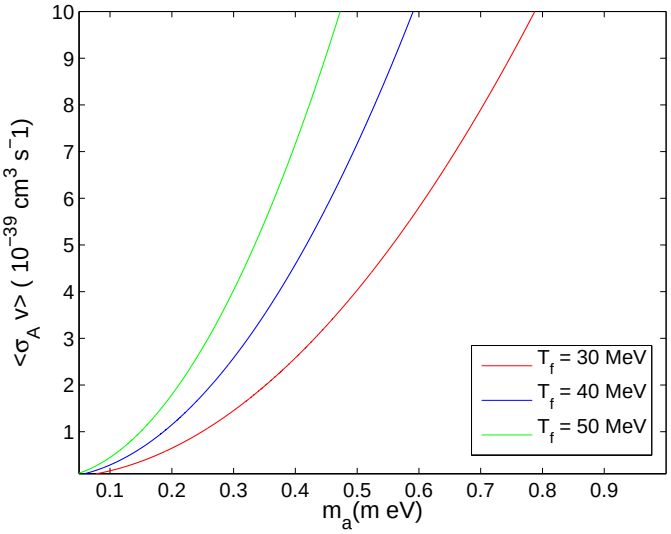

Figure 4.7: Thermally averaged cross section for pion- axion conversion as a function of axion mass for the freeze- out temperatures $T_f = 30\,MeV$, $T_f = 40\,MeV$ and $T_f = 50\,MeV$.

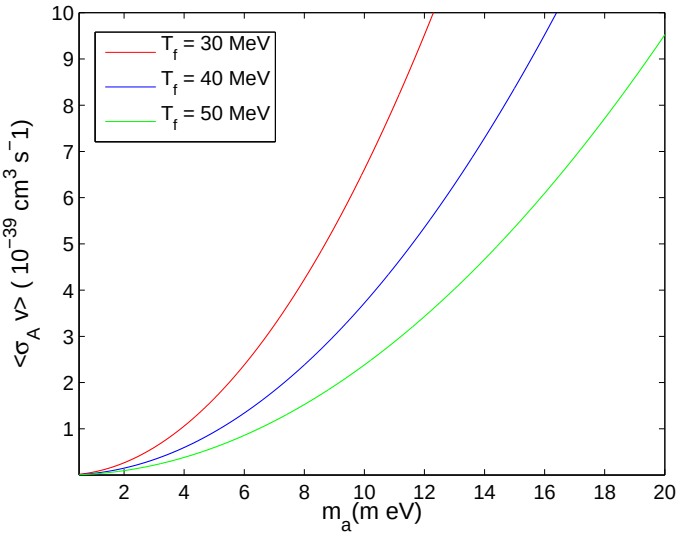

Figure 4.8: Thermally averaged cross section for photo/gluon- production as a function of axion mass for the freeze- out temperatures $T_f = 30\,MeV$, $T_f = 40\,MeV$ and $T_f = 50\,MeV$.

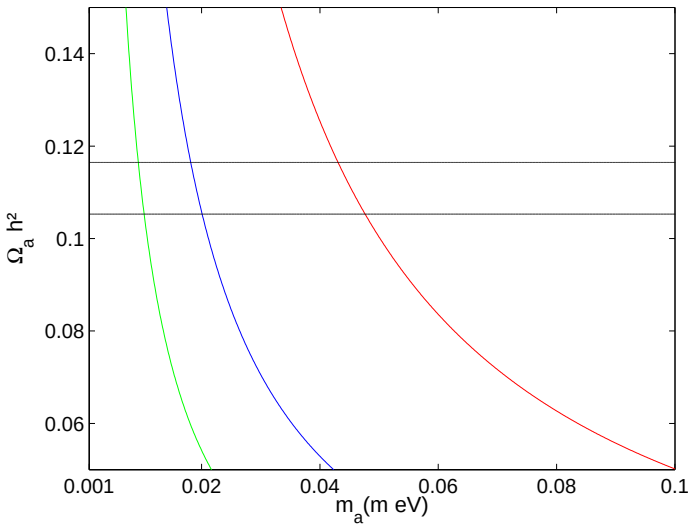

Figure 4.9: Axionic density parameter as a function of axion mass for pion-axion conversion with $g_* = 20.6$. Plot is made for three distinct freeze- out temperatures, $T_f = 30\,\text{MeV}$ (red), $T_f = 40\,\text{MeV}$ (blue) and $T_f = 50\,\text{MeV}$ (green). The two straight lines are the upper and lower bounds from the WMAP-7 data, ref. [6]

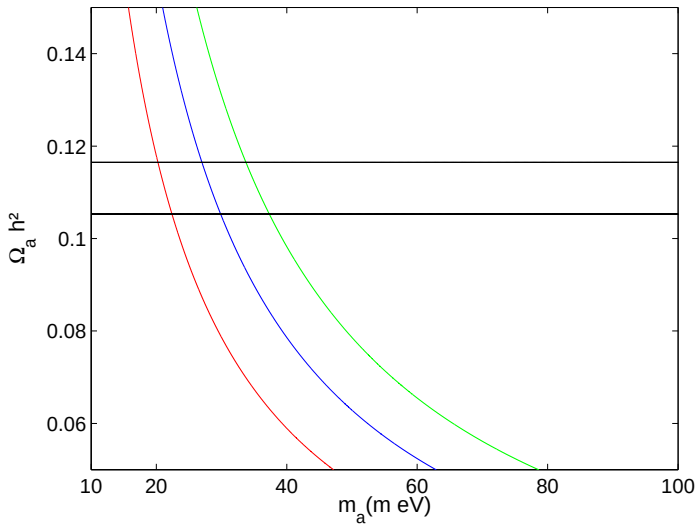

Figure 4.10: Axionic density parameter as a function of axion mass for the axions produced via photo/gluon- production with $g_* = 76.1$.Plot is made for three distinct freeze- out temperatures, $T_f = 30\,\text{MeV}$ (red), $T_f = 40\,\text{MeV}$ (blue) and $T_f = 50\,\text{MeV}$ (green). The two straight lines are the upper and lower bounds from the WMAP-7 data, ref. [6].

4.1.2 Non-thermal production

Axions are produced the non- thermally through the relaxation of the $\overline{\theta}$- in the misalignment mechanism and by radiation of cosmic axions strings.

Misalignment mechanism

The interpretation of axions as the phase of a new scalar field, Φ, allows one to follow the axion field through its cosmic evolution. We will now take a brief qualitative look at the evolution of the axion field in the inflationary scenario, that is assuming inflation occurs.

When the temperature of the universe falls below the Peccei- Quinn scale f_{PQ}, the scalar field develops a vacuum expectation value $\langle\Phi\rangle = (f_{PQ}/\sqrt{2})\, e^{i\,a/f_{PQ}}$. The phase of the scalar field, a/f_{PQ}, will generally vary with location. Since $T \gg \Lambda_{QCD}$ the potential $V(a)$ is so small that there is no energetic difference between various regions in the universe with different values for the axion field in the range $0 \leq a \leq 2\pi f_a$.

After this epoch, inflation (explained in section 1.3.5) is assumed to occur. The result is that only a small portion of the universe becomes our observable region and one certain initial value of the axion field pertains in this region, while other regions are characterized by other values. As the universe expands and cools to temperatures near Λ_{QCD}, the potential $V(a)$ begins to develop:

The axion field is driven toward its equilibrium value at $a = 0$. When the temperature decreases to Λ_{QCD} there is a spontaneous symmetry breaking of the Peccei-Quinn symmetry, $U_{PQ}(1)$, corresponding to the QCD phase transition. What happens is that the Mexican hat potential *tilts*, meaning it changes according to which direction the axion field *chooses* to descend from the equilibrium value at the top of the hat (recall the example of spontaneous symmetry breaking given in section 1.5.4).

If the axion mass $m_a(T)$ becomes larger than the expansion rate of the universe $H(T)$, the axion field goes down towards the minimum of the potential and starts oscillating around it. If the expansion rate were much larger than the axion mass, the axion field would never be able to reach its minimum. At the QCD phase transition a mass term appears for the axion which therefore starts contributing to the matter density of the universe.

4.1.3 Topological structures: cosmic axion strings and domain walls

In the absence of inflation, or if the universe is reheated beyond f_a after inflation, the evolution of the axion field would differ very much from the one outlined

in the previous section. When the temperature of the universe falls below f_a the axion field settles somewhere in the *brim* of its Mexican hat potential. The field would then have different values $a_i(x)$ in different regions of space. In contrast to the inflationary scenario, the different regions of space now remains causally connected and the values a_i vary over several periods. Since only values in the range $0 \leq a \leq 2\pi f_a$ correspond to physically different states, topological defects form, around which the axion field varies by one period. These are 1- dimensional consentrations of energy called cosmic strings.

Because of the large tension in the strings, they will rapidly oscillate and in the process radiate axions. Emission of axions is the major damping mechanism occurring until one straight string remains per horizon volume. String radiation is the dominant source of cosmic axions and it continues until the QCD phase transition occurs. This is when all the previously produced axions develop a mass and start contributing to the matter density of the universe. Also, at this time the explicit breaking of PQ symmetry causes the axion field around strings to collapse into domain walls. A domain wall is a 2- dimensional topological defect.

In this noninflationary scenario the axion production by cosmic string radiation is not an additional source for axions beyond the coherent field oscillations discussed in the "Inflationary scenario"- section, rather it is the only source. Previous discussions of the coherent process are meaningless for the noninflationary scenario. Attempts to calculate the cosmic axion density from coherent oscillations with some averaged value for a_i are therefore useless.

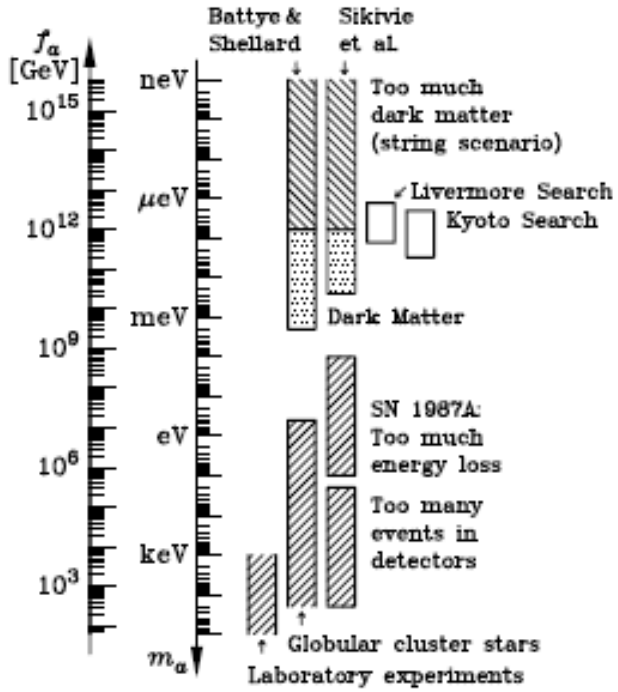

Figure 4.11: Astrophysical and cosmological bounds on axions. One globular cluster limit (white exclusion bar) is based on the axion- electron coupling and thus applies only if axions are of the DFSZ type ($\cos^2\beta = 1$ was used). For the coupling to photons $\zeta = 1$ was assumed. Slanted ends of exclusion bars indicate an estimated uncertainty of the bounds. The cosmological bound from Sikivie et al. was not discussed in this text. Figure courtesy G. Raffelt [1].

Chapter 5

Summary and conclusions

The main purpose of this thesis was to obtain astrophysical and cosmological bounds on the dark matter candidate, the axion.

In the introduction we gave a review of the underlaying physics necessary. A brief outline of stellar structure and evolution was included for the understanding of the astrophysical aspects. The short introduction to general relativity with its applications in cosmology, and to quantum field theory with its applications to particle physics, were all needed for the cosmological aspects.

The axion was introduced properly in chapter 2 through the Peccei- Quinn theory, as the solution of the strong CP problem. We studied its interaction with matter and the different axion models were presented and used for the determination of the model dependent PQ charges.

Next, the energy- loss argument for different processes of stellar evolution were applied in order to obtain constraints on the axion mass m_a and coupling constant f_a. For axions interacting with electrons, the most restrictive bound was obtained from the delay of helium ignition in low- mass red giants. The bound for the axion mass was $m_a C_e \lesssim 0.003\,\text{eV}$. In hadronic axion models, the model-dependent PQ charge, $C_e = 0$. For the DFSZ model, the resulting bound on the axion mass was $m_a cos^2\beta \lesssim 10\,\text{meV}$. The parameter $cos^2\beta$, defined in eq. 2.15, reflects the ratio of the vacuum expectation values of two Higgs fields.

The duration of helium burning in low- mass stars give rise to the most restrictive bound on the axion- photon interaction. From the Primakoff emission of axions a resulting bound obtained on the axion mass was $m_a\,\zeta \lesssim 0.4\,\text{eV}$, where the model dependent parameter ζ is defined in terms of the quark mass ratios in eq. 2.33. In the DFSZ model, $\zeta \approx 1$, so that $m_a \lesssim 0.4\,\text{eV}$.

For the interactions of axions with nucleons, the most restrictive bound is de-

rived from the duration of the neutrino signal of the well studied supernova SN 1987 A. The result obtained was $0.01\,\text{eV} \lesssim m_a \lesssim 10\,\text{eV}$. All the bounds were also stated in terms of the axion decay constant. A summary of the astrophysical constraints is shown in figure 4.1.3.

In the last chapter, the present axion density parameter $\Omega_a h^2$ was derived from the standard WIMP scenario, for axions produced before and after the QCD phase transition. We compared it to the density parameter of CDM given in the 7-year WMAP data, and obtained a bound on the axion mass m_a which also depends on the freeze- out temperature T_f and the effective number of degrees of freedom g_*.

The resulting bound on the axion mass in terms of freeze- out temperature, for axions produced before the QCD phase transition, is shown in figure 4.3. The results are given for an effective relativistic degrees of freedom of $g_* = 20.6$. For a freeze- out temperature of $T_f = 40\,\text{MeV}$, the bound on the axion mass becomes $1.8 \times 10^{-2}\,\text{meV} < m_a < 2.0 \times 10^{-2}\,\text{meV}$. For axions produced after the QCD phase transition, the results are shown in figure 4.4, with $g_* = 76.1$. In this case, we found a bound on m_a for $T_f = 40\,\text{MeV}$ of $26.9\,\text{meV} < m_a < 29.8\,\text{meV}$.

We see that the results suggests an axion mass of order $m_a \sim O(\text{meV})$, hence a corresponding decay constant of order $f_a \sim O(10^{10}\,\text{GeV})$.

Things for the future

When deriving cosmological bounds of the axion through the standard WIMP scenario, we made an assumption that leaves room for improvement. In order to solve the differential equation 4.6, the thermally averaged cross section, $\langle \sigma_A v \rangle$, was assumed to be constant of temperature. Lateron, we used cross section of different temperature dependency for the two scenarios of temperature above and below T_{QCD}.

Bibliography

[1] Georg G. Raffelt. *Stars as Laboratories for Fundamental Physics*. The University of Chicago Press, 1996.

[2] Ostlie Dale A. Carroll, Bradley W. *An Introduction to Modern Astrophysics*. Addison Wesley Publishing Company, 2006.

[3] Dina Prialnik. *An Itroduction to the Theory of Stellar Structure and Evolution*. Cambridge University Press, 2000.

[4] S. Dodelson. *Modern cosmology*. Academic Press, 2003.

[5] Øyvind Grøn. *Lecture Notes on the General Theory of Relativity*. Springer Science+Business Media, 2009.

[6] D. Larson et al. Seven-Year Wilkinson Microwave Anisotropy Probe (WMAP) Observations: Power Spectra and WMAP-Derived Parameters. *Astrophys. J. Suppl.*, 192:16, 2011.

[7] P. Coles and F. Lucchin. *Cosmology. The Origin and Evolution of Cosmic Structure*. John Wiley and Sons, Ltd, 2002.

[8] Øystein Elgarøy. *Lecture Notes in Cosmology*. 2006.

[9] A. R. Liddle. *An Introduction to Modern Cosmology*. Wiley, 2003.

[10] Thomas S. Coleman and Matts Roos. Effective degrees of freedom during the radiation era. *Phys. Rev. D*, 68(2):027702, Jul 2003.

[11] E.W. Kolb and M.S. Turner. *The Early Universe*. Frontiers in physics. Westview Press, 1994.

[12] Olivier Wantz and E. P. S. Shellard. Axion Cosmology Revisited. *Phys. Rev.*, D82:123508, 2010.

[13] Georg G. Raffelt. Astrophysical methods to constrain axions and other novel particle phenomena. *Phys. Rept.*, 198:1–113, 1990.

[14] Georg G. Raffelt. Axions: Recent searches and new limits. pages 419–431, 2005.

[15] Y. Aoki, Z. Fodor, S. D. Katz, and K. K. Szabo. The QCD transition temperature: Results with physical masses in the continuum limit. *Phys. Lett.*, B643:46–54, 2006.

[16] Martin Alan. D. Halzen, F. *Quarks and Leptons: An introductory Course in Modern Particle physics*. John Wiley and Sons,, 1984.

[17] Viatcheslav Mukhanov. *Physical Foundations of Cosmology*. Cambridge University Press, 2005.

[18] R. D. Peccei and Helen R. Quinn. Constraints Imposed by CP Conservation in the Presence of Instantons. *Phys. Rev.*, D16:1791–1797, 1977.

[19] Helen R. Quinn. The CP puzzle in the strong interactions. 2001.

[20] Jihn E. Kim. Weak Interaction Singlet and Strong CP Invariance. *Phys.Rev.Lett.*, 43:103, 1979.

[21] Jihn E. Kim. Light Pseudoscalars, Particle Physics and Cosmology. *Phys. Rept.*, 150:1–177, 1987.

[22] Michael Dine, Willy Fischler, and Mark Srednicki. A Simple Solution to the Strong CP Problem with a Harmless Axion. *Phys. Lett.*, B104:199, 1981.

[23] Zuber Jean-Bernard Itzykson, Claude. *Quantum Field Theory*.

[24] Sanghyeon Chang and Kiwoon Choi. Hadronic axion window and the big-bang nucleosynthesis. *Phys. Lett.*, B316:51–56, 1993.

[25] Shaw G. Mandl, F. *Quantum Field Theory*. John Wiley and Sons,, 1984.

[26] D. McMahon. *Quantum field theory demystified*. McGraw- Hill, 2008.

[27] Sean M. Carroll. *An Introduction to General Relativity, Spacetime and Geometry*. Addison Wesley, 2004.

[28] Georg G. Raffelt. Astrophysical axion bounds. *Lect.Notes Phys.*, 741:51–71, 2008.

[29] Georg G. Raffelt. Axions in astrophysics and cosmology. 1995.

[30] Georg Raffelt. Stellar evolution limits on axion properties. *Nucl.Phys.Proc.Suppl.*, 72:43–53, 1999.

[31] Michael S. Turner. Thermal Production of Not SO Invisible Axions in the Early Universe. *Phys.Rev.Lett.*, 59:2489, 1987.

[32] Michael S. Turner. Cosmic and Local Mass Density of Invisible Axions. *Phys.Rev.*, D33:889–896, 1986.

[33] Michael S. Turner. Windows on the Axion. *Phys.Rept.*, 197:67–97, 1990.

[34] Duane A. Dicus, Edward W. Kolb, Vigdor L. Teplitz, and Robert V. Wagoner. Astrophysical Bounds on the Masses of Axions and Higgs Particles. *Phys. Rev.*, D18:1829, 1978.

[35] Robert J. Scherrer and Michael S. Turner. On the relic, cosmic abundance of stable, weakly interacting massive particles. *Phys. Rev. D*, 33(6):1585–1589, Mar 1986.

[36] Georg G. Raffelt. Astrophysical axion bounds diminished by screening effects. *Phys. Rev.*, D33:897, 1986.

[37] Daniel Grin, Tristan L. Smith, and Marc Kamionkowski. Axion constraints in non-standard thermal histories. *Phys. Rev.*, D77:085020, 2008.

[38] Luca Visinelli and Paolo Gondolo. Axion cold dark matter revisited. *J.Phys.Conf.Ser.*, 203:012035, 2010.

[39] Luca Visinelli and Paolo Gondolo. Dark Matter Axions Revisited. *Phys.Rev.*, D80:035024, 2009.

[40] Paolo Gondolo and Graciela Gelmini. Cosmic abundances of stable particles: Improved analysis. *Nucl.Phys.*, B360:145–179, 1991.

[41] Mark Srednicki, Richard Watkins, and Keith A. Olive. Calculations of Relic Densities in the Early Universe. *Nucl.Phys.*, B310:693, 1988.

[42] Peter Graf and Frank Daniel Steffen. Thermal axion production in the primordial quark-gluon plasma. *Phys.Rev.*, D83:075011, 2011.

[43] David J. Gross, Robert D. Pisarski, and Laurence G. Yaffe. QCD and Instantons at Finite Temperature. *Rev. Mod. Phys.*, 53:43, 1981.

[44] Takeo Moroi and Hitoshi Murayama. Axionic hot dark matter in the hadronic axion window. *Phys.Lett.*, B440:69–76, 1998.

[45] Eduard Masso, Francesc Rota, and Gabriel Zsembinszki. On axion thermalization in the early universe. *Phys.Rev.*, D66:023004, 2002.

[46] Helen R. Quinn. The Symmetry, or lack of it, between matter and antimatter. *Int.J.Mod.Phys.*, A17S1:137–156, 2002.

[47] L.F. Abbott and P. Sikivie. A Cosmological Bound on the Invisible Axion. *Phys.Lett.*, B120:133–136, 1983.

[48] John Preskill, Mark B. Wise, and Frank Wilczek. Cosmology of the Invisible Axion. *Phys.Lett.*, B120:127–132, 1983.

[49] Pierre Sikivie. Axion Cosmology. *Lect.Notes Phys.*, 741:19–50, 2008.

[50] P. Sikivie. Of Axions, Domain Walls and the Early Universe. *Phys.Rev.Lett.*, 48:1156–1159, 1982.

[51] Steen Hannestad, Jan Hamann, Alessandro Mirizzi, Georg G. Raffelt, and Yvonne Y.Y. Wong. Cosmological axion bounds. pages 141–144, 2009.

[52] Steen Hannestad, Alessandro Mirizzi, and Georg Raffelt. New cosmological mass limit on thermal relic axions. *JCAP*, 0507:002, 2005.

[53] Alessandro Melchiorri. A cosmological bound on the thermal axion mass. *Nucl.Phys.Proc.Suppl.*, 194:100–104, 2009.

[54] R.A. Battye and E.P.S. Shellard. Recent perspectives on axion cosmology. pages 554–579, 1997.

[55] E.P.S. Shellard and R.A. Battye. Cosmic axions. 1997.

[56] E.P.S. Shellard and R.A. Battye. On the origin of dark matter axions. *Phys.Rept.*, 307:227–234, 1998.

[57] S. F. Novaes. Standard model: An Introduction. 1999.

[58] A. A. Natale. Introduction to the Standard Model. Presented at 14th Jorge Andre Swieca Summer School, Campos do Jordao, Brazil, 23 Jan - 3 Feb 2007.

[59] Michael Dine. The Utility of quantum field theory. pages 205–220, 2000.

[60] R.A. Battye and E.P.S. Shellard. Axion string constraints. *Phys.Rev.Lett.*, 73:2954–2957, 1994.

[61] R.A. Battye and E.P.S. Shellard. Global string radiation. *Nucl.Phys.*, B423:260–304, 1994.

[62] A.-C. Davis and T.W.B. Kibble. Fundamental cosmic strings. *Contemp.Phys.*, 46:313–322, 2005.

[63] M.B. Hindmarsh and T.W.B. Kibble. Cosmic strings. *Rept.Prog.Phys.*, 58:477–562, 1995.

[64] Hans Arnold Winther. Chameleon Models with Field- dependent Couplings. Master's thesis, the University of Oslo, 2010.

[65] Eirik Gjerløv. On a Controversy Regarding Primordial Gravitational Waves. Master's thesis, the University of Oslo, 2010.